Human Molecular Genetics, 2014, Vol. 23, No. 12 **3200–3211**
doi:10.1093/hmg/ddu030
Advance Access published on January 25, 2014

Clinical whole-genome sequencing in severe early-onset epilepsy reveals new genes and improves molecular diagnosis

Hilary C. Martin[1,†], Grace E. Kim[2,†], Alistair T. Pagnamenta[1,3], Yoshiko Murakami[4], Gemma L. Carvill[5], Esther Meyer[6,7], Richard R. Copley[1,3], Andrew Rimmer[1], Giulia Barcia[8], Matthew R. Fleming[2], Jack Kronengold[2], Maile R. Brown[2], Karl A. Hudspith[1,3], John Broxholme[1], Alexander Kanapin[1], Jean-Baptiste Cazier[1], Taroh Kinoshita[4], Rima Nabbout[8], The WGS500 Consortium[‡], David Bentley[9], Gil McVean[1], Sinéad Heavin[10], Zenobia Zaiwalla[11], Tony McShane[12], Heather C. Mefford[5], Deborah Shears[13], Helen Stewart[13], Manju A. Kurian[6], Ingrid E. Scheffer[10], Edward Blair[13], Peter Donnelly[1,¶], Leonard K. Kaczmarek[2,¶] and Jenny C. Taylor[1,3,¶,*]

[1]Wellcome Trust Centre for Human Genetics, University of Oxford, Oxford, UK, [2]Departments of Cellular and Molecular Physiology and Pharmacology, Yale University School of Medicine, New Haven, CT, USA, [3]NIHR Biomedical Research Centre, Oxford, UK, [4]Department of Immunoregulation, Research Institute for Microbial Diseases, Osaka University, Osaka, Japan, [5]Department of Pediatrics, Division of Genetic Medicine, University of Washington, Seattle, WA, USA, [6]Neurosciences Unit, UCL-Institute of Child Health, London, UK, [7]Department of Neurology, Great Ormond Street Hospital, London, UK, [8]Department of Paediatric Neurology, Centre de Reference Epilepsies Rares, Hôpital Necker-Enfants Malades, Paris, France, [9]Illumina Inc., San Diego, CA, USA, [10]Departments of Medicine and Paediatrics, Florey Institute, The University of Melbourne, Austin Health and Royal Children's Hospital, Melbourne, VIC, Australia, [11]Department of Clinical Neurophysiology, John Radcliffe Hospital, Oxford, UK, [12]Department of Paediatrics, Children's Hospital Oxford, John Radcliffe Hospital, Oxford, UK and [13]Department of Clinical Genetics, Oxford University Hospitals NHS Trust, Oxford, UK

Received September 20, 2013; Revised and Accepted January 20, 2014

In severe early-onset epilepsy, precise clinical and molecular genetic diagnosis is complex, as many metabolic and electro-physiological processes have been implicated in disease causation. The clinical phenotypes share many features such as complex seizure types and developmental delay. Molecular diagnosis has historically been confined to sequential testing of candidate genes known to be associated with specific sub-phenotypes, but the diagnostic yield of this approach can be low. We conducted whole-genome sequencing (WGS) on six patients with severe early-onset epilepsy who had previously been refractory to molecular diagnosis, and their parents. Four of these patients had a clinical diagnosis of Ohtahara Syndrome (OS) and two patients had severe non-syndromic early-onset epilepsy (NSEOE). In two OS cases, we found *de novo* non-synonymous mutations in the genes *KCNQ2* and *SCN2A*. In a third OS case, WGS revealed paternal isodisomy for chromosome 9, leading to identification of the causal homozygous missense variant in *KCNT1*, which produced a substantial increase in potassium channel current. The fourth OS patient had a recessive mutation in *PIGQ* that led to exon skipping and defective glycophosphatidyl inositol biosynthesis. The two patients with NSEOE had likely pathogenic *de novo* mutations in *CBL* and *CSNK1G1*, respectively. Mutations in these

*To whom correspondence should be addressed at: Genomic Medicine Theme, Oxford Biomedical Research Centre, Wellcome Trust Centre for Human Genetics, Oxford OX3 7BN, UK. Tel: +44 1865287633; Fax: +44 1865287770; Email: jenny@well.ox.ac.uk
†These authors contributed equally to this work.
‡A full list of members is provided in the Supplementary Material.
¶These authors jointly directed this work.

genes were not found among 500 additional individuals with epilepsy. This work reveals two novel genes for OS, *KCNT1* and *PIGQ*. It also uncovers unexpected genetic mechanisms and emphasizes the power of WGS as a clinical tool for making molecular diagnoses, particularly for highly heterogeneous disorders.

INTRODUCTION

Many recent studies have successfully used whole-exome or whole-genome sequencing (WES, WGS) to uncover the genetic basis of rare disorders (reviewed by 1,2), primarily in a research context. In addition, WES and WGS offer potentially revolutionary approaches to molecular diagnosis for patients in a clinical setting. In order to assess the possible clinical utility of WGS, we have sequenced the genomes of 500 individuals with a variety of medical conditions, including cancer, immunological disease and rare, putatively monogenic syndromes (3–5). As part of this 'WGS500 project', we sequenced six patients with severe early-onset epilepsy who had been previously refractory to molecular diagnosis.

Severe early-onset epilepsy is a good candidate for WGS as it is a challenging disorder to understand mechanistically. It represents a broad spectrum of phenotypes which are highly heterogeneous at the clinical and molecular levels (6). While some causative genes have been identified for many of these subphenotypes, the limitations of current technologies mean that genetic testing is largely confined to the genes associated with the specific presenting phenotype. However, it is increasingly being recognized that a given gene can cause multiple phenotypes (6), and that more comprehensive genetic testing may improve molecular diagnostic yield (7). This is useful clinically not only because it can help make or confirm a diagnosis, but also because it may allow counseling on recurrence risk and prenatal testing.

In its most severe form, early-onset epilepsy involves frequent seizures beginning in the first three months of life, with abundant epileptic activity that contributes to significant cognitive and motor delay (6,8). It is frequently associated with gross structural brain abnormalities and occasionally with metabolic disorders, which are often genetic in origin (9). Ohtahara Syndrome (OS) is a severe form of early-onset epilepsy characterized by a distinctive electroencephalogram (EEG) pattern known as 'burst-suppression', which consists of periodic high voltage bursts of slow waves mixed with spikes, followed by marked attenuation (10). The frequency of OS is about 1 in 100 000 live births (11). Children with OS typically have multiple seizure types including tonic spasms and focal seizures, which are often refractory to anti-epileptic drugs (12). Affected children may progress onto other epilepsy syndromes such as West Syndrome (6), or they may die in infancy.

Several genes have been implicated in severe early-onset epilepsy. The first reported for OS was the X-linked *ARX* gene, which encodes a developmental transcription factor (13). *De novo* mutations in *STXBP1* (14,15), encoding a protein involved in synaptic vesicle release, in *CDKL5* (16), encoding a serine/threonine kinase, and in ion channel genes *KCNQ2* (17), *SCN2A* (18,19) and *SCN8A* (20) have also been implicated, as have recessive mutations in the glutamate transporter *SLC25A22* (21). However, many OS patients test negative for mutations in these genes, indicating that other genes have yet to be identified. Multiple additional genes have been associated with the broader range of early-onset epilepsies, including genes encoding cytoskeletal components [*SPTAN1* (22)] and proteins involved in signaling [*PLCB1* (23)], DNA repair [*PNKP* (24)] and neurotransmitter synthesis [*PNPO* (25)]. However, clinical testing is limited by the availability and costs of conventional single-gene tests, and thus tends to be restricted to genes that have been associated with the specific type of epilepsy. There is therefore scope to apply a more comprehensive approach to diagnosis using whole-genome methods.

In this study, we sequenced six patients with sporadic severe early-onset epilepsy, and their healthy parents. The patients were selected because traditional clinical molecular genetic approaches had failed to uncover the causal mutation. Four of the children had been diagnosed with OS, and two had severe non-syndromic early-onset epilepsy (NSEOE). Because these six cases were all sporadic, and the families were reported as non-consanguineous, we anticipated that the causal mutation was most likely to be *de novo*, but we also considered the simple, compound and X-linked recessive models.

RESULTS

We sequenced the six trios (Table 1; Supplementary Materials, Note S1) to high coverage on the Illumina HiSeq platform. In searching for the causal mutations, we considered coding variants as well as variants in regulatory regions within 50 kb of known early-onset epilepsy genes (see Materials and Methods). The most plausible causal variant in each trio was a coding mutation, and we report these here. See the Supplementary Materials, Note S2 for a description of candidate variants that were not deemed to be causal.

Patients 1 and 3: *KCNQ2* and *SCN2A*

Two OS cases had *de novo* non-synonymous mutations in genes encoding ion channel subunits, *KCNQ2* and *SCN2A* (Table 1; Supplementary Materials, Fig. S1A and B). The *KCNQ2* mutation, NM_004518:c.C827T:p.T276I, falls in the highly conserved fifth transmembrane segment of the channel that forms part of the pore. It is two amino acids away from the T274M mutation recently described in an OS patient (26). The *SCN2A* mutation in Patient 3, NM_001040143:c.A5558G:p.H1853R, is in the cytosolic C-terminal region of the protein. It falls within the 250 residue domain that binds FGF14, which is required for localization at the axon initial segment (27). Other *de novo* mutations in the cytosolic domains were recently reported in patients with OS (18). These reports provide strong supporting evidence that these *de novo* mutations, which have not been previously reported in any epilepsy patients, are responsible for OS in these children.

Table 1. Phenotypes and presumed causal mutations in the six trios sequenced

Trio	Phenotype	Age of seizure onset	Current age	Family history	Previous genetic tests	Brain MRI	EEG	Presumed causal mutation	Evidence for pathogenicity
1	OS; severe DD	1 day	5 years	No	arrayCGH, *FRAXA, STXBP1, MECP2, CDKL5, POLG, ARX*	Age 14 days: reduced posterior white matter volume; thin corpus callosum	Age 14 days: Burst suppression	*de novo* in *KCNQ2*: NM_004518:c.C827T: p.T276I	*KCNQ2* previously implicated in OS
2	OS; metopic synostosis; severe DD	1 day	4 years	Paternal great-grandmother and her sister had epilepsy	arrayCGH, *FRAXA*, *MECP2*, *CDKL5*, *STXBP1*	Age 1 year: cerebral atrophy with delayed myelination and hypomyelination	Age 14 days: Burst suppression	Recessive variant in *KCNT1*, homozygous due to UPD9: NM_020822: c.G2896A:p.A966T	*KCNT1* previously implicated in MMPSI and ADNFLE; electrophysiology demonstrated effect on channel current
3	OS; severe DD	14 days	5 years	No	arrayCGH, *CDKL5*, *ARX*, *STXBP1*	Age 8 months: cerebral atrophy, delayed & reduced myelination	Age 6 weeks: Burst suppression	*de novo* in *SCN2A*: NM_001040143: c.A5558G:p.H1853R	*SCN2A* previously implicated in OS
4	OS; severe DD	4 weeks	Deceased age 2 years, 4 months	Mother's cousin died of seizures at age 2	arrayCGH, *MECP2*, *ARX*, *STXBP1*	Age 9 months: delayed and reduced myelination	Age 3 months: Burst suppression	Simple recessive in *PIGQ*: NM_004204:exon3: c.690-2A>G	Binding partner *PIGA* implicated in similar syndrome; mutation leads to exon skipping and reduced GPI synthesis
5	Severe NSEOE; microcephaly; severe DD	2 days	19 years	No	arrayCGH, *MECP2*, *UBE3A*, *TCF4*	Microcephalic (OFC <3rd percentile); structurally normal brain	Age 8 years: multifocal seizure potential on background of significant disruption of cortical function	*de novo* in *CSNK1G1*: NM_022048:c.C688T: p.R230W	*CSNK1G1* involved in synaptic transmission
6	Severe NSEOE; severe DD; PDA and ASD as neonate; cutaneous hypopigmentation	2.5 months	11 years	No	arrayCGH, *MECP2*, *CDKL5*, *STXBP1*	Cerebral hypoplasia; microcephaly (OFC < 0.4th percentile)	Age 6 years: background diffusely of low amplitude, with multifocal sharp waves	*de novo* in *CBL*: NM_005188:exon9: c.1228-1G>A	*CBL* implicated in NCFC syndrome; mutation leads to exon skipping

OS, Ohtahara syndrome; NSEOE, non-syndromic early-onset epilepsy; DD, developmental delay; PDA, patent ductus arteriosis; ASD, atrial septal defect; OFC, occipital frontal cortex; MMPSI, malignant migrating partial seizures of infancy; ADNFLE, autosomal dominant nocturnal frontal lobe epilepsy; GPI, glycosylphosphatidyl inositol; NCFC, neuro-cardio-facial-cutaneous; UPD, uniparental disomy. More detailed clinical descriptions, including seizure types, head circumference and treatments, are given in Supplementary Materials, Note S1.

Patient 2: *KCNT1*

Patient 2 had very severe early-onset epilepsy, an EEG consistent with OS (Supplementary Material, Fig. S2), and profound developmental delay. He had a paternal family history of childhood idiopathic epilepsy affecting his father's maternal aunt, grandmother and nephew. Patient 2 did not have any compelling *de novo* mutations. However, low chromosomal heterozygosity and detection of multiple Mendelian errors (Fig. 1; Supplementary Materials, Fig. S1C) suggested that he had paternal isodisomy for chromosome 9. This was subsequently confirmed by SNP array (Supplementary Materials, Fig. S3; see Supplementary Materials, Note S3). This finding prompted two new alternative hypotheses: that the patient's symptoms were due to aberrant expression of an imprinted gene on chromosome 9, or that there was a recessive pathogenic mutation on this chromosome that had become homozygous as a result of the isodisomy. There was no evidence in the literature for imprinted genes on this chromosome that had plausible links to epilepsy. We therefore scanned the patient's chromosome 9 for rare homozygous

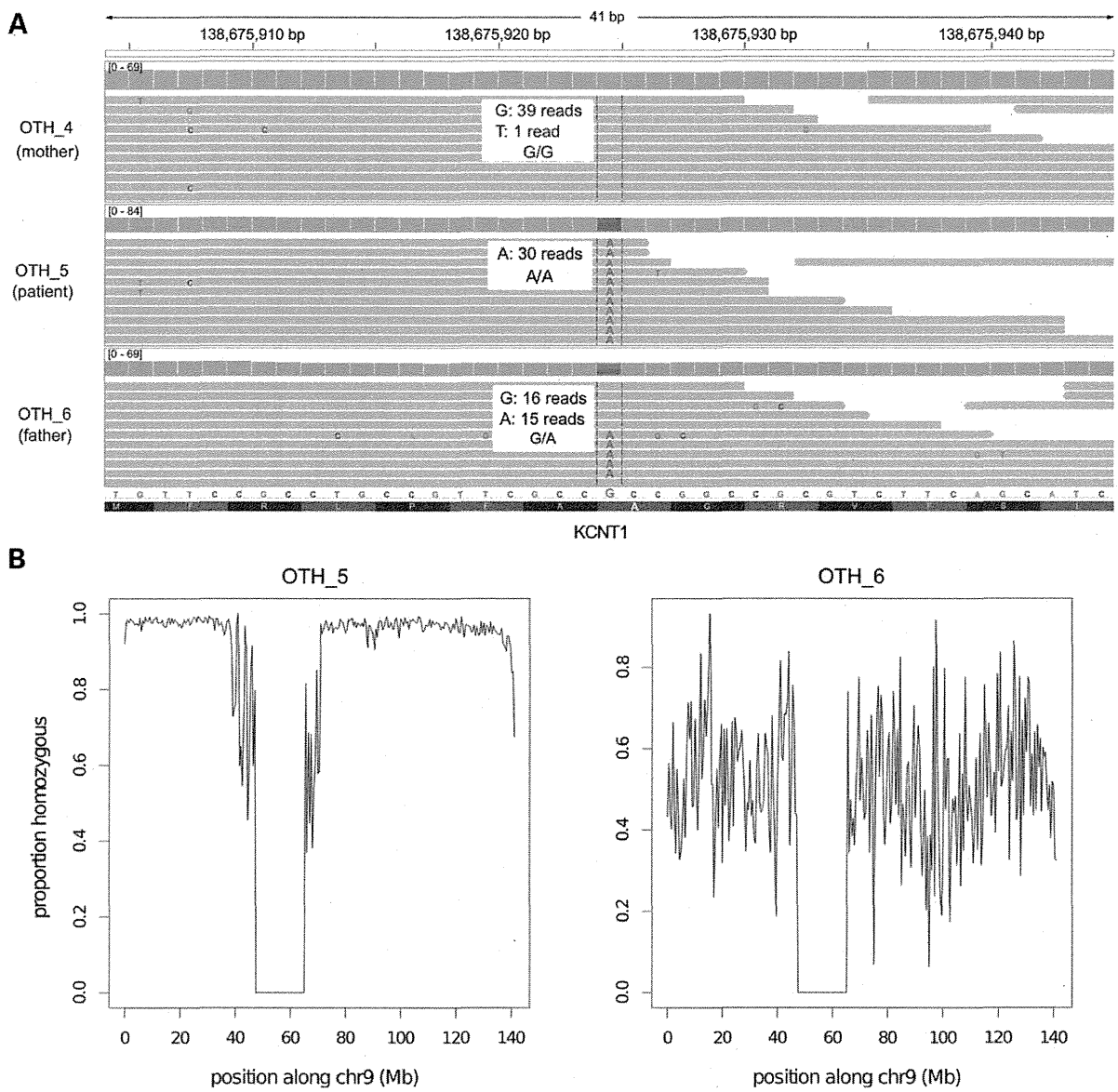

Figure 1. Paternal isodisomy in Patient 2. (**A**) We observed multiple Mendelian errors on chromosome 9 which led us to suspect uniparental disomy (UPD). All variants in the patient (OTH_5) appeared to have been inherited from his father (OTH_6). The *KCNT1* variant is illustrated here as an example. Grey bars represent individual sequencing reads from the sample indicated on the left, and colored letters divergences from the reference sequence. The grey 'pile-up' along the top indicates the sequence coverage. The genotype of each individual is shown. (**B**) These plots show the proportion of variants that are homozygous in 500 kb windows across chr9. OTH_5 was completely homozygous, apart from a few spurious calls; the pattern is similar to that seen on chromosome X in males. His father, OTH_6, is shown for comparison. Note that the dip in the middle represents the centromere.

variants that might be pathogenic, including around *STXBP1* and *SPTAN1*. The only plausible candidate was a novel non-synonymous variant in *KCNT1* at 9q34.3 that disrupted a highly conserved alanine residue in the intracellular C-terminal domain, NM_020822:c.G2896A:p.A966T. This gene encodes the Na^+-activated K^+ channel known as 'Slack', which is very widely expressed throughout the brain (28). Dominant mutations in *KCNT1* were recently reported to cause autosomal dominant nocturnal frontal lobe epilepsy (ADNFLE) (29), malignant migrating partial seizures of infancy (MMPSI) (30,31) and infantile spasms (32). Interestingly, one of the MMPSI patients with a *KCNT1* mutation was described as having a 'subtle' burst-suppression EEG (30). Distinct from this patient, however, our Patient 2 did not have migrating seizures, and had a clear burst-suppression EEG pattern. Thus, different mutations in *KCNT1* have heterogeneous phenotypic consequences.

The A966 residue in *KCNT1* is completely conserved across all vertebrates for which genome sequences are available. The sequence of the Slack channel C-terminal region is highly conserved between rat and human (92% identical), and residue A966 in the human Slack channel corresponds to residue A945 in the rat protein. We therefore used a rat mutant construct to explore the effect of the novel mutation on channel function, in the same way we described previously for the MMPSI-linked R428Q and A934T mutations (31). We expressed wild-type (WT) and A945T rat Slack in *Xenopus laevis* oocytes, and measured channel activity by performing two-electrode voltage clamping experiments. These experiments showed that activity of the A945T mutant channel was increased significantly by a factor of 13 relative to the WT at +60 mV (Fig. 2A and B). The amounts and integrity of the WT and A945T cRNA used in these experiments appeared similar, just 8% higher in the mutant than the WT (Fig. 2C).

Slack channel activity increases with depolarization (28,33). We therefore compared the voltage dependence of A945T and WT channels. Channel activity of the A945T mutant was significantly greater than that of the WT at all positive potentials (Fig. 2D). However, the voltage dependence of activation of the A945T mutant with depolarization to positive potentials did not differ from that of the WT channel (Fig. 2D) or from that of the previously published reports of Slack channel voltage dependence (31,33). Together, these results suggest that channel opening probability may be greater in the A945T than the WT channel over the same range of depolarized membrane potentials, which would account for the epileptic activity seen in this patient.

Patient 4: *PIGQ*

Patient 4, who was of West African origin, had severe early-onset epilepsy with a burst-suppression EEG, consistent with OS. Although he was reported to be non-consanguineous,

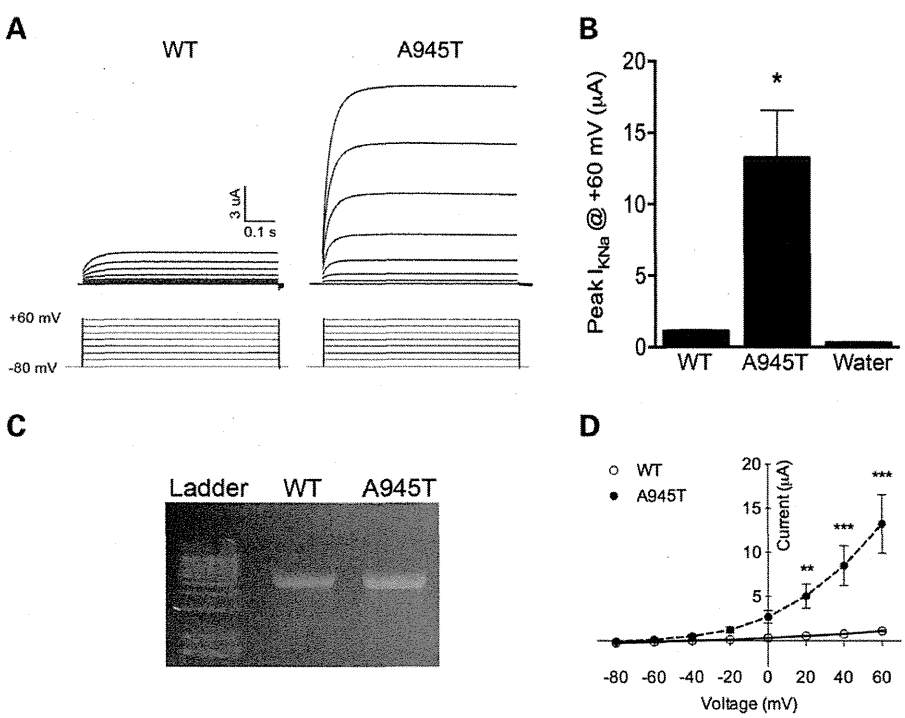

Figure 2. Electrophysiological and channel expression analysis of *KCNT1* mutation found in Patient 2. WT or A945T mutant Slack channel was expressed in *Xenopus laevis* oocytes, and two-electrode voltage clamping (TEVC) performed. (**A**) A representative trace of current activity recorded from an oocyte expressing WT or A945T is shown on top, with the voltage-clamping protocol displayed underneath. (**B**) Averaged quantitation of the peak current is compared at +60 mV ($P < 0.001$, $n = 5$, Student's *t*-test; representative of three independent experiments). (**C**) The quality of RNA injected into *Xenopus* oocytes was checked on a 1% formaldehyde agarose gel. (**D**) Current–voltage relations for the WT or A945T channels. Channel activity as measured at peak current amplitude and normalized to the value at +60 mV is plotted against voltage ($^{**}P < 0.01$, $^{***}P < 0.001$, $n = 5$, two-way ANOVA, Sidak's multiple comparisons test).

we found several extended homozygous regions in his genome. Within a 2 Mb homozygous region on chr16, he had a novel homozygous single nucleotide variant (SNV) that was predicted to disrupt the highly conserved splice acceptor site of exon 3 of the *PIGQ* gene: NM_004204:exon3:c.690−2A>G. Both parents were heterozygous and two unaffected siblings were either heterozygous or homozygous for the reference allele (Supplementary Materials, Fig. S1D). *PIGQ*, formerly called *GPI1*, encodes a subunit of an *N*-acetylglucosaminyltransferase that catalyzes the first step in glycosylphosphatidyl inositol (GPI) biosynthesis. *PIGQ* stabilizes the enzyme complex (34). A nonsense mutation in the X-linked *PIGA* gene, which encodes another subunit of this enzyme, was recently reported to cause a lethal disorder characterized by multiple congenital abnormalities, structural brain malformations, joint contractures and neonatal seizures with a burst-suppression EEG (35). Recessive mutations in other GPI synthesis genes cause clinically heterogeneous syndromes, all of which involve seizures (36–39). Thus, this *PIGQ* mutation seemed a very plausible candidate for causing OS in Patient 4.

The patient died before we discovered this mutation so we were unable to obtain samples to test the effect of this homozygous mutation on *PIGQ* activity. However, we obtained RNA samples from his parents' blood and examined *PIGQ* splicing. There were two *PIGQ* transcripts, one consistent with the reference annotation and another with a deletion of exon 3, as expected given that the parents were heterozygous for the variant at the splice acceptor site for this exon (Fig. 3A; Supplementary Materials, Fig. S4). Since exon 3 falls immediately before the catalytic domain of *PIGQ*, the mutation seemed likely to abrogate the function of the enzyme and lead to a reduction in GPI synthesis, as was seen for the nonsense mutation in *PIGA* (35). We tested the parents for abnormalities in serum alkaline phosphatase levels and in expression of CD59 on red blood cells, which are typical signs of impaired GPI synthesis (35,36,40), but found none. This is not entirely surprising since heterozygous carriers of other *PIG* gene mutations had normal CD59 levels (37).

The skipping of exon 3 causes an in-frame deletion of 44 amino acids (Fig. 3A). To assess whether this abnormality affected PIGQ function *in vitro*, we transfected human *PIGQ* cDNA either with or without exon 3 into *PIGQ*-deficient Chinese hamster ovary (CHO) cell lines. The mutant *PIGQ* did not restore the surface expression of GPI-anchored proteins (GPI-AP) as efficiently as the WT (Fig. 3B). Additionally, the expression of mutant protein was greatly decreased to a level undetectable by western blotting (Fig. 3C). These results demonstrated that the PIGQ protein lacking the 44 amino acids had some functional activity but was unstable, and so GPI synthesis was impaired. Over 150 proteins have been reported to have GPI anchors (41), including several with important roles in neural development and function (42–44). Further work is needed to determine which of these provides the causal link with epilepsy.

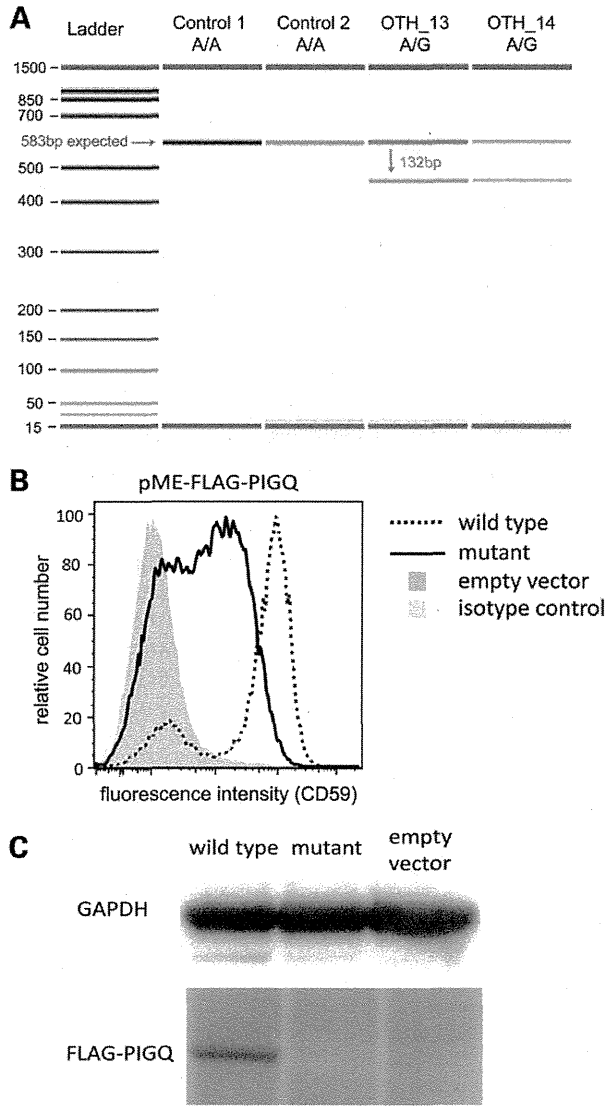

Figure 3. PIGQ splicing mutation in Patient 4. (**A**) The variant causes skipping of exon 3. This image shows the Bioanalyzer gel from an RT-PCR (see Materials and Methods) and demonstrates the presence of two PIGQ transcripts in the heterozygous parents (OTH_13, OTH_14). The blue arrow indicates the band expected from the annotated transcript, and the red arrow that expected from the skipping of exon 3. (**B**) Severely decreased functional activity of the mutant *PIGQ*. *PIGQ*-deficient CHO cells were transiently transfected with WT or mutant *PIGQ* cDNA (lacking exon 3). Restoration of the surface expression of CD59, a GPI-anchored protein, was assessed by flow cytometry after staining with anti-CD59 antibody. The mutant *PIGQ* did not restore the surface expression of CD59 as efficiently as the WT. X axis, fluorescence intensity corresponding to CD59 expression level per cell; Y axis, relative cell number. (**C**) The expression of mutant protein was greatly decreased and could not be detected by western blotting.

Patient 5: *CSNK1G1*

Patient 5 had severe tonic-clonic epilepsy, microcephaly and developmental delay. We found a *de novo* non-synonymous mutation at a highly conserved site in *CSNK1G1* (NM_022048: c.C688T:p.R230W; Supplementary Materials, Fig. S1E). This gene encodes casein kinase 1 (CK1), gamma 1, a serine/threonine kinase expressed in many tissues including the brain. CK1 regulates the phosphorylation of NMDA receptors and is thus important for synaptic transmission (45) (see Supplementary Materials, Note S4). The *CSNK1G1* mutation is a prime

candidate in this patient, but genetic validation studies did not find any additional patients (see below) and further work is needed to definitively establish it as causal.

Patient 6: *CBL*

Patient 6 had severe tonic epilepsy, microcephaly and developmental delay. We detected a *de novo* mutation in a highly conserved splice site in the *CBL* gene (NM_005188:exon9: c.1228-1G>A), and showed that this led to exon skipping (Supplementary Materials, Fig. S5). Cbl is a ubiquitously expressed adaptor molecule and ubiquitin ligase that regulates the Ras/MAPK pathway (46). It is primarily recognized as a tumor suppressor (47), but germline mutations in it and other genes involved in the Ras/MAPK pathway can also cause various developmental disorders collectively known as the neuro-cardio-facial-cutaneous (NCFC) syndromes or 'RASopathies' (48). Notably, mutations in *KRAS* and *BRAF* were recently reported in two boys with refractory epilepsy and cardio-facial-cutaneous (CFC) syndrome (49). It is likely that this splicing mutation ablates Cbl's ubiquitin ligase activity, thereby over-stimulating Ras/MAPK signaling. This may have disrupted neuronal development and led to severe epilepsy (more details in Supplementary Materials, Note S4).

The patient was reviewed by a number of clinical geneticists. Hypopigmented skin lesions and a history of congenital heart disease were noted, but the clinical diagnosis of a NCFC was not considered likely. Review after this molecular finding did not affect the clinical diagnosis and this patient is still thought not to fit phenotypically into this group of disorders. If this gene is confirmed to be causal, this will widen further the phenotype of the Ras-MAPK disorders.

Mutation screening in other cases

Using a targeted resequencing approach (50), we screened *KCNT1*, *PIGQ*, *CBL* and *CSNK1G1* in a large cohort of epileptic encephalopathy cases from Australia (Supplementary Materials, Table S1). This included two cases of OS, five of early myoclonic encephalopathy [EME; a syndrome which shares features with OS but which is predominantly myoclonic in nature (51)], and thirty-eight of early-onset epileptic encephalopathy (defined as onset within the first three months of life). We also screened these genes in thirteen other cases of OS and EME (Supplementary Materials, Table S2) from a UK cohort, using Sanger sequencing. We looked for coding variants that would fit a recessive model in *KCNT1* and *PIGQ*, or a *de novo* model in *CBL* and *CSNK1G1*, as was observed in our patients, but found none. Two of the OS cases have subsequently been attributed to mutations in other genes (50). Thus, our failure to replicate our findings likely reflects further genetic heterogeneity in severe early-onset epilepsy. We also appreciate the relatively small number of patients we have screened who had similar phenotypes to those described here (total sixteen OS, six EME).

DISCUSSION

WGS heralds promise as a tool for clinical diagnosis of patients with genetic disease. As part of a wide-ranging program to evaluate the clinical utility of WGS (WGS500), we sequenced six patients with severe early-onset epilepsy who had evaded molecular diagnosis by conventional single-gene clinical screening. In doing so, we identified two new genes for OS, as well as two putative genes for severe early-onset epilepsy. This increases the number of known genes for OS from six [*STXBP1* (14), *ARX* (13), *CDKL5* (16), *KCNQ2* (26), *SCN2A* (18) and *SLC25A22* (52)] to eight (adding *KCNT1* and *PIGQ*). In two cases, we found an unexpected inheritance mechanism: uniparental disomy of chromosome 9 in Patient 2, and simple recessive inheritance due to likely distant consanguinity in Patient 4.

Of particular interest was the discovery that Patient 2 had a pathogenic mutation in *KCNT1* that became homozygous through isodisomy. To date, there have been two published cases of homozygous mutations due to isodisomy causing syndromes involving seizures (53,54), but no examples of such mutations causing severe epilepsy. This is also the first reported case of paternal isodisomy for chromosome 9, and of an apparently recessive mutation in *KCNT1*; recently reported mutations causing MMPSI (31), ADNFLE (29) and infantile spasms (55) were all dominant. Nevertheless, we note that, while this mutation appears to be acting in a recessive manner, there was a paternal history of mild idiopathic epilepsy. It is possible that, in the heterozygous state, this variant predisposes to milder epilepsy, but further testing of affected family members was not possible.

The Slack *KCNT1* A945T mutation had a gain-of-function effect on channel activity. Although the two previously characterized MMPSI-causing mutations, R409Q and A913T, were also gain-of-function alterations, the A945T mutation appears to have a much more profound effect. Whereas channel activity was increased by a factor of 3 at +60 mV in the two MMPSI mutant channels (31), the corresponding increase was 13-fold for the A945T mutation. This observation raises the possibility that the patterns of neuronal firing that produce the distinctive EEG patterns characteristic of these different disorders can vary as a function of *KCNT1* channel activity, and can furthermore influence the nature, severity and onset of the seizures.

The *PIGQ* finding emphasizes the importance of the GPI pathway in brain development and function. This gene was not initially considered as a candidate, since the patient did not have the congenital abnormalities found in children with other *PIG* gene mutations, such as polydactyly. However, it became a very plausible candidate after its binding partner, *PIGA*, was reported to cause a lethal disorder involving neonatal seizures (35). We then demonstrated that the *PIGQ* mutation impairs GPI synthesis in a similar manner (Fig. 3). It remains an open question as to how defective GPI synthesis causes epilepsy, although a number of mechanisms have been suggested, including impaired *Cripto* signaling leading to aberrant forebrain development (44), and disruption of contactin-mediated organization of axonal subdomains at the node of Ranvier (42).

We have also made some unexpected findings about the etiology of other non-syndromic forms of early-onset epilepsy. Although the mutations in patients 5 and 6 have not been definitively established as causal, our results point to several interesting pathways not generally associated with epilepsy. The *de novo* splicing mutation in *CBL* in Patient 6 implies that this patient's condition is actually a 'RAS-opathy' (56), which may be consistent with her congenital heart disease. Other genes in the Ras/MAPK pathway have been reported to cause

epileptic encephalopathy (49) but *CBL* has not. It has been implicated as a cause of juvenile myelomonocytic leukemia (57,58) and also of a Noonan-like syndrome with microcephaly (57,59). A clinical review after our discovery confirmed that Patient 6 did not have facial features typical of Noonan syndrome. Thus, our results suggest that *CBL* mutations may give rise to an even wider spectrum of phenotypes than previously thought.

Our discovery of the *de novo* non-synonymous *CSNK1G1* mutation in Patient 5 hints that the epileptogenic mechanism may involve the Wnt pathway, which CK1 regulates (60,61), although disruptions in synaptic transmission due to abnormal phosphorylation of NMDA receptors (45) would be a more direct explanation. Intriguingly, the *Drosophila* homolog of *CSNK1G3* was found to suppress seizures in the Na^+-channel gain-of-function mutant $para^{bss1}$ (62). Also, a mutation in *PRICKLE1*, which encodes a regulator of the Dishevelled proteins that are intracellular transducers of Wnt signals (63), has been reported to cause progressive myoclonic epilepsy (61). For both *CBL* and *CSNK1G1*, causality can only be definitely established by finding other mutations in patients with similar phenotypes or by extensive functional work in model organisms. Identifying and screening cases similar to Patient 6, rather than those with a more typical NCFC clinical presentation, may increase the chance of finding further patients with *CBL* mutations.

Other groups have already demonstrated the power of WES and WGS in rapidly pinpointing novel genes underlying a rare disease (1,64), particularly in the case of *de novo* inheritance (65). Although all the cases described in this article could probably have been solved by WES, which would have been considerably cheaper, there is emerging evidence to suggest that WES misses clinically relevant mutations because of unequal or incomplete coverage of exons, particularly around the exon boundaries (66). Given that two of our mutations were in splice sites, this was especially relevant. Additionally, the ability to check for pathogenic non-coding mutations in WGS data, as we have done around known early-onset epilepsy genes, is an additional benefit of this approach.

Our study underlines the significant potential of WGS for providing rapid clinical diagnosis of patients with heterogeneous genetic diseases. The patients being investigated here had undergone numerous genetic, biochemical and imaging tests over many years but had been refractory to diagnosis. Using WGS, three of the six patients (Patients 1–3) received a confirmed molecular diagnosis in a clinically relevant timeframe. Conventional molecular testing would not have included these genes. *KCNT1* had not previously been implicated in OS and would not therefore have been tested for this specific phenotype, even though it was described for other severe epilepsy phenotypes after we started this project (29,31). Similarly, *KCNQ2* and *SCN2A* had only been described for benign seizures (67,68) until recent reports of association with the more severe OS phenotype (17,18). These results have already improved the clinical management of these patients' families by providing informed and accurate reproductive risk counseling and the prospect of prenatal diagnosis for future pregnancies.

For the remaining three patients, candidate mutations likely to cause their epilepsy have been identified. The evidence is particularly strong for *PIGQ*, since a homozygous nonsense mutation in *PIGA* causes a similar phenotype (35), and we demonstrated that our mutation was loss of function. Further genetic and functional validation work is required to prove causality definitively, and this remains a challenge in a clinical setting, particularly for rare diseases. Nevertheless, this situation is expected to improve with greater adoption of these technologies and increased sharing of genetic data in public databases.

In conclusion, our results have led to identification of novel genes for severe epilepsy phenotypes and, in addition, demonstrate the clinical utility of WGS as a means of providing comprehensive and rapid molecular diagnosis for patients with mechanistically complex genetic diseases, with concomitant implications for clinical management of these disorders.

MATERIALS AND METHODS

Description of patients

The six patients were recruited through the Oxford Clinical Genetics department. A summary of the main clinical features is given in Table 1, along with a list of the genetic tests they had undergone before entering this study (all of which were negative). All patients also had extensive metabolic tests on blood, urine and cerebral spinal fluid, all of which were normal. A more detailed clinical description is given in Supplementary Materials, Note S1.

Read mapping and variant calling

WGS was conducted on the Illumina HiSeq platform to a coverage of at least 25×. The reads were mapped to the human reference genome (build 37d5) with Stampy (69), and SNVs and small indels were called with an in-house algorithm, Platypus (70). Variants were annotated relative to RefSeq transcripts using ANNOVAR (71) and relative to all Ensembl transcripts using an in-house tool called VariantAnno.

Variant filtering strategy

To identify *de novo* mutations in the trios, we first screened for variants that were called as homozygous reference in the parents but heterozygous in the child. We then filtered these based on the genotype likelihood ratio (the difference between the log likelihoods for the most likely and the second most likely genotypes), requiring this to be below −5 in all three individuals. This left an average of 126 candidate *de novo* mutations in each trio [about 70 being expected given a mutation rate of 1.18×10^{-8} per base pair per generation (72)]. To remove those likely to be due to technical artifacts or incorrect calling of parental genotypes, we removed variants that had been seen before in WGS500, the 1000 Genomes Project or the NHLBI Exome Sequencing Project (ESP). We then prioritized variants that were predicted to alter the protein sequence in any transcript (non-synonymous SNVs, stop loss or gain variants, indels or splice site mutations), particularly those that were highly conserved across the 46 vertebrate species in the UCSC conservation track. There were 0–3 candidate *de novo* coding mutations per trio.

We also considered a simple recessive or compound heterozygous model in all families, as well as an X-linked model where appropriate. For the compound heterozygous model, we required

two coding variants in the same gene, one inherited from each heterozygous parent. Since EOEE is extremely rare (frequency ~1/100 000), we excluded variants with a frequency greater than 0.005 in 1000 Genomes or ESP, or for which there were any homozygotes or hemizygotes or more than five heterozygotes among the other WGS500 samples ($n = 294$), which included no other patients with seizures.

In addition to screening for coding variants, we also looked for variants that might be affecting regulation of known EOEE genes. Specifically, we focused on variants at conserved positions in regulatory regions within 50 kb of the candidate genes *KCNQ2, SCN2A, SCN1A, SPTAN1, SRGAP2, MAGI1, PLCB1, STXBP1, PNPO, PCDH19, GRIN2A, MAPK10, CDKL5, SLC25A22, ERBB4* and *ARX*. A variant was considered conserved if it had a GERP (73) or phyloP (74) score greater than 2 or a phastCons (75) score greater than 0.95, or was in a GERP constrained element (73) or a phastCons constrained element (75). We used the regulatory regions defined by the Ensembl V65 Regulatory Build (http://www.ensembl.org/info/genome/funcgen/regulatory_build.html, last accessed date on February, 2013).

Variant validation

All putatively causal variants were Sanger-sequenced to confirm the genotypes of the proband and parents.

Splicing assays

Fresh blood was collected using PAXgene blood RNA tubes (Becton Dickinson, Oxford, UK) and RNA was extracted using the PAXgene Blood RNA kit (Qiagen). cDNA was synthesized using the QuantiTect Reverse Transcription kit (Qiagen) according to the manufacturer's instructions. We carried out a PCR using the FastStart Kit (Roche) and primers as follows: PIGQ-2F, CACGCAGTGAGGTGCTCTT; PIGQ-5R, GGGGACATGAGGTGGATGTA; CBL-8F, GAGATGGGCTCCACATTCC; CBL-11R, GAACTTGGGGCAGATACTGG. To size PCR products accurately, we used 'on-chip-electrophoresis' and ran 1 μl on a DNA 1000 v2.3 chip using the 2100 Bioanalyser system (Agilent). We expected WT RT-PCR products of 583 and 698 bp for NM_004204 (*PIGQ*) and NM_005188 (*CBL*), respectively. Sanger sequencing was used to confirm the identity of the aberrant bands.

KCNT1 functional work

Site-directed mutagenesis and cRNA synthesis

The rat homologue (A945T) of the human *KCNT1* A966T mutation was created using the QuikChange Mutagenesis kit (Stratagene) using the WT *KCNT1* construct in pOX expression vector as the template, and the following primers: 5′-GTTCCGCCTGCCATTTGCTACTGGTCGGGTGTTTAGTA-3′ (forward) and 5′-TACTAAACACCCGACCAGTAGCAAATGGCAGGCGGAAC-3′ (reverse). The resulting construct was sequenced to confirm the presence of mutation. The cDNA construct was then linearized using NotI, and the complementary RNA (cRNA) made using the mMessage mMachine T3 kit (Ambion). The final reaction was purified using MinElute PCR Purification kit (Qiagen), and RNA eluted in nuclease-free water. RNA purity and concentration was checked using a NanoDrop reader. RNA quality was also checked on a 1% formaldehyde agarose gel, and its densitometry quantitated using ImageJ to confirm its concentration. cRNA was stored at −20°C until ready for use.

Electrophysiological characterization in Xenopus laevis *oocytes*

All animal procedures were approved by the IACUC at Yale University. Oocytes were prepared as described previously (31). Defolliculated oocytes were injected with 10 ng of RNA encoding WT or A966T, or with sterile water. Oocytes were kept at 18°C, and two-electrode voltage clamping was performed on days 2–5 post-injection, as reported previously (31,76).

PIGQ functional work

We used a previously described human *PIGQ* expression vector (77). The *PIGQ* mutant construct lacking exon 3 was made by site-directed mutagenesis. *PIGQ*-deficient CHO cells (10.2.1) (78) were transiently transfected with FLAG-tagged WT or mutant *PIGQ* cDNA, driven by an SRα promoter (pME FLAG-PIGQ) together with a luciferase expression plasmid for monitoring transfection efficiency. Two days later, to determine the restoration of GPI-AP expression, cells were stained with anti-CD59 (5H8) antibody followed by phycoerythrin-conjugated anti-mouse IgG, and analyzed by a flow cytometer (Cant II; BD Biosciences, Franklin Lakes, NJ, USA) using the Flowjo software (Tommy Digital Inc., Tokyo, Japan). To determine FLAG-tagged *PIGQ* protein levels, lysates of transfected cells were subjected to SDS–PAGE, and western blotting was performed using anti-FLAG antibody (M2, Sigma, St Louis, MO, USA), with anti-GAPDH (6C5, Life Technologies, Carlsbad, CA, USA) as a loading control. Transfection efficiency was determined by luciferase activity using the Luciferase assay kit (Promega, Madison, WI, USA).

Screening candidate genes in Australian cohort

We sequenced *PIGQ*, *CSNK1G1*, *CBL* and *KCNT1* in a cohort of 500 epileptic encephalopathy patients from Australia. These patients had a variety of different phenotypes, the breakdown of which is shown in Supplementary Materials, Table S1, with an age of onset ranging from 1 day to 25 years.

We used Molecular Inversion Probes (MIPs) to capture all exon and intron/exon boundaries (5 bp flanking) of target genes (Refseq, hg19 build). Detailed methodology is described elsewhere (79). Briefly, pooled MIPs (Supplementary Materials, Table S3) were used to capture target exons from 100 ng of each proband's DNA and target enrichment was performed by PCR using unique reverse primers for each DNA sample. Pooled libraries were subject to massively parallel sequencing using a 101 paired-end protocol on a HiSeq.

We performed raw read processing as described (79), but use a modified analysis pipeline for variant calling. SNV and indel calling and filtering was performed using the Genome Analysis Tool Kit (GATK version 2.2) (http://www.broadinstitute.org/gatk/, last accessed date on February, 2013). We excluded from further analysis any variants with allele balance >0.70,

QUAL < 30, QD < 5 or coverage < 25×, and variants in clusters (window size 10 bp) or in homopolymer runs (5 bp). Variants were annotated with SeattleSeq (version 134; http://snp.gs.washington.edu/SeattleSeqAnnotation134/) and the Exome Sequencing Project dataset (see http://eversusgs.washington.edu/EVS/, last accessed date on February, 2013) used to assess variant frequency in the control population. For dominant (or *de novo*) models, we considered only variants not present in this control sample set. For recessive candidates, we considered variants with a frequency in controls of <1% (European American control frequency). Only non-synonymous, splice-site or frameshift variants were assessed further.

Where family members were available, segregation analysis was performed using a 'MIP-pick' strategy. We selected and re-pooled only the MIPs that captured the genomic sequence harboring the rare variant of interest and performed target enrichment PCR and sequencing as above for all relevant probands and family members.

Screening candidate genes in UK cases

We carried out Sanger sequencing of *CBL*, *CSNK1G1*, *PIGQ* and *KCNT1* in 11 patients with Ohtahara syndrome. Clinical details are given in Supplementary Materials, Table S2. Genomic DNA from participating individuals was extracted from peripheral lymphocytes by standard techniques. All participants gave written informed consent and the study was performed in accordance with the Declaration of Helsinki.

Primer pairs were designed for all coding exons with primer3 software (1,2) (http://bioinfo.ut.ee/primer3/, last accessed date on February, 2013) (Supplementary Materials, Table S4). The exons were amplified by PCR using BioMix™ Red (Bioline Ltd). Two different PCR conditions were carried out to amplify exons: (i) an initial denaturation of 95°C for 5 min, followed by 35 cycles of 45 s denaturation at 95°C, 45 s annealing at 58–62°C (depending on fragment) and 1 min extension at 72°C with a final extension at 72°C for 5 min, or (ii) a touchdown PCR program: an initial denaturation of 95°C for 5 min, followed by 24 cycles of 30 s denaturation at 95°C, 30 s annealing at 62°C (minus 0.5°C per cycle) and 1 min extension at 72°C, followed by 15 cycles of 30 s denaturation at 95°C, 30 s annealing at 50°C and 1 min extension at 72°C with a final extension at 72°C for 10 min. If PCR condition 1 was not successful, PCR condition 2 was applied. PCR products were cleaned up with MicroCLEAN (Web Scientific) and were directly sequenced by the Big Dye Terminator Cycle Sequencing System (Applied Biosystems Inc.). Sequencing reactions were run on an ABI PRISM 3730 DNA Analyzer (Applied Biosystems Inc.) and analyzed using Chromas (http://www.technelysium.com.au/chromas.html, last accessed date on February, 2013).

AUTHOR CONTRIBUTIONS

H.C.M. analyzed the WGS data. L.K.K. directed the *KCNT1* electrophysiology experiments, which were performed by G.E.K., M.F., M.R.B. and J.K. A.T.P. and K.A.H. did the Sanger sequencing and splicing assays. G.B. made the *KCNT1* construct for electrophysiology, supervised by R.N. J.B., A.K. and J.-B.C. created the bioinformatics infrastructure of the WGS500 project and provided NGS data processing, preparing the BAM files and variant calls. R.C. and A.R. contributed to WGS analysis. Y.M. and T.K. did the *in vitro PIGQ* experiments. S.H. and I.E.S. studied patients in the Australian cohort and performed phenotyping analysis of the larger epilepsy panel, on which G.C. and H.M. performed the MIP sequencing. M.A.K. and E.M. performed phenotyping and Sanger sequencing on the UK cohort. H.S., D.S. and E.B. contributed samples and clinical data from the affected individuals and assisted with the interpretation of results. Z.Z. and T.M. provided clinical data and advice on the phenotypes. E.B., D.B., G.M., J.C.T. and P.D. conceived the study, and L.K.K., E.B., P.D. and J.T. directed it. H.C.M., G.E.K., A.T.P., E.B., I.E.S., L.K.K., J.C.T. and P.D. wrote the article. This project was carried out as part of the WGS500 Consortium.

SUPPLEMENTARY MATERIAL

Supplementary Material is available at *HMG* online.

ACKNOWLEDGEMENTS

We thank the patients and their families for participating in this study, the Genomics Core at the Wellcome Trust Centre for Human Genetics (WTCHG) for generating the WGS data, Elham Sadighi Akha for running the SNP arrays for trio 2 and Kevin Leyden for doing the CD59 flow cytometry assay for trio 4. We are also grateful to Adeline Nogh and Amy McTague for their input in gathering the UCL cohort, and to Helen Cross and Jozef Gecz for facilitating initial contact between groups.

Conflict of Interest statement. D.B. is an employee of Illumina Inc.

FUNDING

This work was supported in part by a Wellcome Trust Core Award (090532/Z/09/Z) to the Wellcome Trust Centre for Human Genetics and a Wellcome Trust Senior Investigator Award to P.D. (095552/2/11/2), in part by NIH grant HD067517 and in part by the Oxford NIHR Biomedical Research Centre. Funding to pay the Open Access publication charges for this article was provided by the wellcome Trust and the Oxford NIHR Biomedical Research Centre.

REFERENCES

1. Bamshad, M.J., Ng, S.B., Bigham, A.W., Tabor, H.K., Emond, M.J., Nickerson, D.A. and Shendure, J. (2011) Exome sequencing as a tool for Mendelian disease gene discovery. *Nat. Rev. Genet.*, **12**, 745–755.
2. Rabbani, B., Mahdieh, N., Hosomichi, K., Nakaoka, H. and Inoue, I. (2012) Next-generation sequencing: impact of exome sequencing in characterizing Mendelian disorders. *J. Hum. Genet.*, **57**, 621–632.
3. Palles, C., Cazier, J.B., Howarth, K.M., Domingo, E., Jones, A.M., Broderick, P., Kemp, Z., Spain, S.L., Almeida, E.G., Salguero, I. *et al.* (2012) Germline mutations affecting the proofreading domains of POLE and POLD1 predispose to colorectal adenomas and carcinomas. *Nat. Genet.*, **45**, 136–144.
4. Lise, S., Clarkson, Y., Perkins, E., Kwasniewska, A., Sadighi Akha, E., Schnekenberg, R.P., Suminaite, D., Hope, J., Baker, I., Gregory, L. *et al.*

(2012) Recessive mutations in SPTBN2 implicate beta-III spectrin in both cognitive and motor development. *PLoS Genet.*, **8**, e1003074.
5. Sharma, V.P., Fenwick, A.L., Brockop, M.S., McGowan, S.J., Goos, J.A., Hoogeboom, A.J., Brady, A.F., Jeelani, N.O., Lynch, S.A., Mulliken, J.B. *et al.* (2013) Mutations in TCF12, encoding a basic helix-loop-helix partner of TWIST1, are a frequent cause of coronal craniosynostosis. *Nat. Genet.*, **45**, 304–307.
6. Nordli, D.R. Jr. (2012) Epileptic encephalopathies in infants and children. *J. Clin. Neurophysiol.*, **29**, 420–424.
7. Kodera, H., Kato, M., Nord, A.S., Walsh, T., Lee, M., Yamanaka, G., Tohyama, J., Nakamura, K., Nakagawa, E., Ikeda, T. *et al.* (2013) Targeted capture and sequencing for detection of mutations causing early onset epileptic encephalopathy. *Epilepsia*, **54**, 1262–1269.
8. Berg, A.T., Berkovic, S.F., Brodie, M.J., Buchhalter, J., Cross, J.H., van Emde Boas, W., Engel, J., French, J., Glauser, T.A., Mathern, G.W. *et al.* (2010) Revised terminology and concepts for organization of seizures and epilepsies: report of the ILAE Commission on Classification and Terminology, 2005–2009. *Epilepsia*, **51**, 676–685.
9. Ohtahara, S. and Yamatogi, Y. (2003) Epileptic encephalopathies in early infancy with suppression-burst. *J. Clin. Neurophysiol.*, **20**, 398–407.
10. Pavone, P., Spalice, A., Polizzi, A., Parisi, P. and Ruggieri, M. (2012) Ohtahara syndrome with emphasis on recent genetic discovery. *Brain Dev.*, **34**, 459–468.
11. Hino-Fukuyo, N., Haginoya, K., Iinuma, K., Uematsu, M. and Tsuchiya, S. (2009) Neuroepidemiology of West syndrome and early infantile epileptic encephalopathy in Miyagi Prefecture, Japan. *Epilepsy Res.*, **87**, 299–301.
12. Tavyev Asher, Y.J. and Scaglia, F. (2012) Molecular bases and clinical spectrum of early infantile epileptic encephalopathies. *Eur. J. Med. Genet.*, **55**, 299–306.
13. Kato, M., Saitoh, S., Kamei, A., Shiraishi, H., Ueda, Y., Akasaka, M., Tohyama, J., Akasaka, N. and Hayasaka, K. (2007) A longer polyalanine expansion mutation in the ARX gene causes early infantile epileptic encephalopathy with suppression-burst pattern (Ohtahara syndrome). *Am. J. Hum. Genet.*, **81**, 361–366.
14. Saitsu, H., Kato, M., Mizuguchi, T., Hamada, K., Osaka, H., Tohyama, J., Uruno, K., Kumada, S., Nishiyama, K., Nishimura, A. *et al.* (2008) De novo mutations in the gene encoding STXBP1 (MUNC18-1) cause early infantile epileptic encephalopathy. *Nat. Genet.*, **40**, 782–788.
15. Deprez, L., Weckhuysen, S., Holmgren, P., Suls, A., Van Dyck, T., Goossens, D., Del-Favero, J., Jansen, A., Verhaert, K., Lagae, L. *et al.* (2010) Clinical spectrum of early-onset epileptic encephalopathies associated with STXBP1 mutations. *Neurology*, **75**, 1159–1165.
16. Melani, F., Mei, D., Pisano, T., Savasta, S., Franzoni, E., Ferrari, A.R., Marini, C. and Guerrini, R. (2011) CDKL5 gene-related epileptic encephalopathy: electroclinical findings in the first year of life. *Dev. Med. Child Neurol.*, **53**, 354–360.
17. Saitsu, H., Kato, M., Koide, A., Goto, T., Fujita, T., Nishiyama, K., Tsurusaki, Y., Doi, H., Miyake, N., Hayasaka, K. *et al.* (2012) Whole exome sequencing identifies KCNQ2 mutations in Ohtahara syndrome. *Ann. Neurol.*, **72**, 298–300.
18. Nakamura, K., Kato, M., Osaka, H., Yamashita, S., Nakagawa, E., Haginoya, K., Tohyama, J., Okuda, M., Wada, T., Shimakawa, S. *et al.* (2013) Clinical spectrum of SCN2A mutations expanding to Ohtahara syndrome. *Neurology*, **81**, 992–998.
19. Touma, M., Joshi, M., Connolly, M.C., Grant, P.E., Hansen, A.R., Khwaja, O., Berry, G.T., Kinney, H.C., Poduri, A. and Agrawal, P.B. (2013) Whole genome sequencing identifies SCN2A mutation in monozygotic twins with Ohtahara syndrome and unique neuropathologic findings. *Epilepsia*, **54**, e81–e85.
20. Veeramah, K.R., O'Brien, J.E., Meisler, M.H., Cheng, X., Dib-Hajj, S.D., Waxman, S.G., Talwar, D., Girirajan, S., Eichler, E.E., Restifo, L.L. *et al.* (2012) De novo pathogenic SCN8A mutation identified by whole-genome sequencing of a family quartet affected by infantile epileptic encephalopathy and SUDEP. *Am. J. Hum. Genet.*, **90**, 502–510.
21. Molinari, F., Raas-Rothschild, A., Rio, M., Fiermonte, G., Encha-Razavi, F., Palmieri, L., Palmieri, F., Ben-Neriah, Z., Kadhom, N., Vekemans, M. *et al.* (2005) Impaired mitochondrial glutamate transport in autosomal recessive neonatal myoclonic epilepsy. *Am. J. Hum. Genet.*, **76**, 334–339.
22. Saitsu, H., Tohyama, J., Kumada, T., Egawa, K., Hamada, K., Okada, I., Mizuguchi, T., Osaka, H., Miyata, R., Furukawa, T. *et al.* (2010) Dominant-negative mutations in alpha-II spectrin cause West syndrome with severe cerebral hypomyelination, spastic quadriplegia, and developmental delay. *Am. J. Hum. Genet.*, **86**, 881–891.
23. Kurian, M.A., Meyer, E., Vassallo, G., Morgan, N.V., Prakash, N., Pasha, S., Hai, N.A., Shuib, S., Rahman, F., Wassmer, E. *et al.* (2010) Phospholipase C beta 1 deficiency is associated with early-onset epileptic encephalopathy. *Brain*, **133**, 2964–2970.
24. Shen, J., Gilmore, E.C., Marshall, C.A., Haddadin, M., Reynolds, J.J., Eyaid, W., Bodell, A., Barry, B., Gleason, D., Allen, K. *et al.* (2010) Mutations in PNKP cause microcephaly, seizures and defects in DNA repair. *Nat. Genet.*, **42**, 245–249.
25. Mills, P.B., Surtees, R.A., Champion, M.P., Beesley, C.E., Dalton, N., Scambler, P.J., Heales, S.J., Briddon, A., Scheimberg, I., Hoffmann, G.F. *et al.* (2005) Neonatal epileptic encephalopathy caused by mutations in the PNPO gene encoding pyridox(am)ine 5′-phosphate oxidase. *Hum. Mol. Genet.*, **14**, 1077–1086.
26. Weckhuysen, S., Mandelstam, S., Suls, A., Audenaert, D., Deconinck, T., Claes, L.R., Deprez, L., Smets, K., Hristova, D., Yordanova, I. *et al.* (2012) KCNQ2 encephalopathy: emerging phenotype of a neonatal epileptic encephalopathy. *Ann. Neurol.*, **71**, 15–25.
27. Laezza, F., Lampert, A., Kozel, M.A., Gerber, B.R., Rush, A.M., Nerbonne, J.M., Waxman, S.G., Dib-Hajj, S.D. and Ornitz, D.M. (2009) FGF14 N-terminal splice variants differentially modulate Nav1.2 and Nav1.6-encoded sodium channels. *Mol. Cell. Neurosci.*, **42**, 90–101.
28. Bhattacharjee, A., Gan, L. and Kaczmarek, L.K. (2002) Localization of the Slack potassium channel in the rat central nervous system. *J. Comp. Neurol.*, **454**, 241–254.
29. Heron, S.E., Smith, K.R., Bahlo, M., Nobili, L., Kahana, E., Licchetta, L., Oliver, K.L., Mazarib, A., Afawi, Z., Korczyn, A. *et al.* (2012) Missense mutations in the sodium-gated potassium channel gene KCNT1 cause severe autosomal dominant nocturnal frontal lobe epilepsy. *Nat. Genet.*, **44**, 1188–1190.
30. McTague, A., Appleton, R., Avula, S., Cross, J.H., King, M.D., Jacques, T.S., Bhate, S., Cronin, A., Curran, A., Desurkar, A. *et al.* (2013) Migrating partial seizures of infancy: expansion of the electroclinical, radiological and pathological disease spectrum. *Brain*, **136**, 1578–1591.
31. Barcia, G., Fleming, M.R., Deligniere, A., Gazula, V.R., Brown, M.R., Langouet, M., Chen, H., Kronengold, J., Abhyankar, A., Cilio, R. *et al.* (2012) De novo gain-of-function KCNT1 channel mutations cause malignant migrating partial seizures of infancy. *Nat. Genet.*, **44**, 1255–1259.
32. Allen, A.S., Berkovic, S.F., Cossette, P., Delanty, N., Dlugos, D., Eichler, E.E., Epstein, M.P., Glauser, T., Goldstein, D.B., Han, Y. *et al.* (2013) De novo mutations in epileptic encephalopathies. *Nature*, **501**, 217–221.
33. Joiner, W.J., Tang, M.D., Wang, L.Y., Dworetzky, S.I., Boissard, C.G., Gan, L., Gribkoff, V.K. and Kaczmarek, L.K. (1998) Formation of intermediate-conductance calcium-activated potassium channels by interaction of Slack and Slo subunits. *Nat. Neurosci.*, **1**, 462–469.
34. Hong, Y., Ohishi, K., Watanabe, R., Endo, Y., Maeda, Y. and Kinoshita, T. (1999) GPI1 stabilizes an enzyme essential in the first step of glycosylphosphatidylinositol biosynthesis. *J. Biol. Chem.*, **274**, 18582–18588.
35. Johnston, J.J., Gropman, A.L., Sapp, J.C., Teer, J.K., Martin, J.M., Liu, C.F., Yuan, X., Ye, Z., Cheng, L., Brodsky, R.A. *et al.* (2012) The phenotype of a germline mutation in PIGA: the gene somatically mutated in paroxysmal nocturnal hemoglobinuria. *Am. J. Hum. Genet.*, **90**, 295–300.
36. Maydan, G., Noyman, I., Har-Zahav, A., Neriah, Z.B., Pasmanik-Chor, M., Yeheskel, A., Albin-Kaplanski, A., Maya, I., Magal, N., Birk, E. *et al.* (2011) Multiple congenital anomalies-hypotonia-seizures syndrome is caused by a mutation in PIGN. *J. Med. Genet.*, **48**, 383–389.
37. Almeida, A.M., Murakami, Y., Layton, D.M., Hillmen, P., Sellick, G.S., Maeda, Y., Richards, S., Patterson, S., Kotsianidis, I., Mollica, L. *et al.* (2006) Hypomorphic promoter mutation in PIGM causes inherited glycosylphosphatidylinositol deficiency. *Nat. Med.*, **12**, 846–851.
38. Krawitz, P.M., Schweiger, M.R., Rodelsperger, C., Marcelis, C., Kolsch, U., Meisel, C., Stephani, F., Kinoshita, T., Murakami, Y., Bauer, S. *et al.* (2010) Identity-by-descent filtering of exome sequence data identifies PIGV mutations in hyperphosphatasia mental retardation syndrome. *Nat. Genet.*, **42**, 827–829.
39. Thompson, M.D., Roscioli, T., Marcelis, C., Nezarati, M.M., Stolte-Dijkstra, I., Sharom, F.J., Lu, P., Phillips, J.A., Sweeney, E., Robinson, P.N. *et al.* (2012) Phenotypic variability in hyperphosphatasia with seizures and neurologic deficit (Mabry syndrome). *Am. J. Med. Genet. A*, **158A**, 553–558.
40. Krawitz, P.M., Murakami, Y., Hecht, J., Kruger, U., Holder, S.E., Mortier, G.R., Delle Chiaie, B., De Baere, E., Thompson, M.D., Roscioli, T. *et al.* (2012) Mutations in PIGO, a member of the GPI-anchor-synthesis pathway,

cause hyperphosphatasia with mental retardation. *Am. J. Hum. Genet.*, **91**, 146–151.
41. Fujita, M. and Kinoshita, T. (2012) GPI-anchor remodeling: potential functions of GPI-anchors in intracellular trafficking and membrane dynamics. *Biochim. Biophys. Acta*, **1821**, 1050–1058.
42. Labasque, M. and Faivre-Sarrailh, C. (2010) GPI-anchored proteins at the node of Ranvier. *FEBS Lett.*, **584**, 1787–1792.
43. Borrie, S.C., Baeumer, B.E. and Bandtlow, C.E. (2012) The Nogo-66 receptor family in the intact and diseased CNS. *Cell Tissue Res.*, **349**, 105–117.
44. McKean, D.M. and Niswander, L. (2012) Defects in GPI biosynthesis perturb Cripto signaling during forebrain development in two new mouse models of holoprosencephaly. *Biol. Open*, **1**, 874–883.
45. Chergui, K., Svenningsson, P. and Greengard, P. (2005) Physiological role for casein kinase 1 in glutamatergic synaptic transmission. *J. Neurosci.*, **25**, 6601–6609.
46. Swaminathan, G. and Tsygankov, A.Y. (2006) The Cbl family proteins: ring leaders in regulation of cell signaling. *J. Cell. Physiol.*, **209**, 21–43.
47. Kales, S.C., Ryan, P.E., Nau, M.M. and Lipkowitz, S. (2010) Cbl and human myeloid neoplasms: the Cbl oncogene comes of age. *Cancer Res.*, **70**, 4789–4794.
48. Denayer, E. and Legius, E. (2007) What's new in the neuro-cardio-facial-cutaneous syndromes? *Eur. J. Pediatr.*, **166**, 1091–1098.
49. Adachi, M., Abe, Y., Aoki, Y. and Matsubara, Y. (2012) Epilepsy in RAS/MAPK syndrome: two cases of cardio-facio-cutaneous syndrome with epileptic encephalopathy and a literature review. *Seizure*, **21**, 55–60.
50. Carvill, G.L., Heavin, S.B., Yendle, S.C., McMahon, J.M., O'Roak, B.J., Cook, J., Khan, A., Dorschner, M.O., Weaver, M., Calvert, S. *et al.* (2013) Targeted resequencing in epileptic encephalopathies identifies de novo mutations in CHD2 and SYNGAP1. *Nat. Genet.*, **45**, 825–830.
51. Djukic, A., Lado, F.A., Shinnar, S. and Moshe, S.L. (2006) Are early myoclonic encephalopathy (EME) and the Ohtahara syndrome (EIEE) independent of each other? *Epilepsy Res.*, **70** (Suppl. 1), S68–S76.
52. Molinari, F. (2010) Mitochondria and neonatal epileptic encephalopathies with suppression burst. *J. Bioenerg. Biomembr.*, **42**, 467–471.
53. Vantaggiato, C., Redaelli, F., Falcone, S., Perrotta, C., Tonelli, A., Bondioni, S., Morbin, M., Riva, D., Saletti, V., Bonaglia, M.C. *et al.* (2009) A novel CLN8 mutation in late-infantile-onset neuronal ceroid lipofuscinosis (LINCL) reveals aspects of CLN8 neurobiological function. *Hum. Mutat.*, **30**, 1104–1116.
54. Gumus, H., Ghesquiere, S., Per, H., Kondolot, M., Ichida, K., Poyrazoglu, G., Kumandas, S., Engelen, J., Dundar, M. and Caglayan, A.O. (2010) Maternal uniparental isodisomy is responsible for serious molybdenum cofactor deficiency. *Dev. Med. Child Neurol.*, **52**, 868–872.
55. Allen, A.S., Berkovic, S.F., Cossette, P., Delanty, N., Dlugos, D., Eichler, E.E., Epstein, M.P., Glauser, T., Goldstein, D.B., Han, Y. *et al.* (2013) De novo mutations in epileptic encephalopathies. *Nature*, **501**, 217–221.
56. Zenker, M. (2011) Clinical manifestations of mutations in RAS and related intracellular signal transduction factors. *Curr. Opin. Pediatr.*, **23**, 443–451.
57. Niemeyer, C.M., Kang, M.W., Shin, D.H., Furlan, I., Erlacher, M., Bunin, N.J., Bunda, S., Finklestein, J.Z., Sakamoto, K.M., Gorr, T.A. *et al.* (2010) Germline CBL mutations cause developmental abnormalities and predispose to juvenile myelomonocytic leukemia. *Nat. Genet.*, **42**, 794–800.
58. Perez, B., Mechinaud, F., Galambrun, C., Ben Romdhane, N., Isidor, B., Philip, N., Derain-Court, J., Cassinat, B., Lachenaud, J., Kaltenbach, S. *et al.* (2010) Germline mutations of the CBL gene define a new genetic syndrome with predisposition to juvenile myelomonocytic leukaemia. *J. Med. Genet.*, **47**, 686–691.
59. Martinelli, S., De Luca, A., Stellacci, E., Rossi, C., Checquolo, S., Lepri, F., Caputo, V., Silvano, M., Buscherini, F., Consoli, F. *et al.* (2010) Heterozygous germline mutations in the CBL tumor-suppressor gene cause a Noonan syndrome-like phenotype. *Am. J. Hum. Genet.*, **87**, 250–257.
60. Fossat, N., Jones, V., Garcia-Garcia, M.J. and Tam, P.P. (2012) Modulation of WNT signaling activity is key to the formation of the embryonic head. *Cell Cycle*, **11**, 26–32.
61. Bassuk, A.G., Wallace, R.H., Buhr, A., Buller, A.R., Afawi, Z., Shimojo, M., Miyata, S., Chen, S., Gonzalez-Alegre, P., Griesbach, H.L. *et al.* (2008) A homozygous mutation in human PRICKLE1 causes an autosomal-recessive progressive myoclonus epilepsy-ataxia syndrome. *Am. J. Hum. Genet.*, **83**, 572–581.
62. Howlett, I.C., Rusan, Z.M., Parker, L. and Tanouye, M.A. (2013) Drosophila as a Model for Intractable Epilepsy: Gilgamesh Suppresses Seizures in parabss1 Heterozygote Flies. *G3 (Bethesda)*, **3**, 1399–1407.
63. Chan, D.W., Chan, C.Y., Yam, J.W., Ching, Y.P. and Ng, I.O. (2006) Prickle-1 negatively regulates Wnt/beta-catenin pathway by promoting Dishevelled ubiquitination/degradation in liver cancer. *Gastroenterology*, **131**, 1218–1227.
64. Foo, J.N., Liu, J.J. and Tan, E.K. (2012) Whole-genome and whole-exome sequencing in neurological diseases. *Nat. Rev. Nephrol.*, **8**, 508–517.
65. Veltman, J.A. and Brunner, H.G. (2012) De novo mutations in human genetic disease. *Nat. Rev. Genet.*, **13**, 565–575.
66. Sikkema-Raddatz, B., Johansson, L.F., de Boer, E.N., Almomani, R., Boven, L.G., van den Berg, M.P., van Spaendonck-Zwarts, K.Y., van Tintelen, J.P., Sijmons, R.H., Jongbloed, J.D. *et al.* (2013) Targeted next-generation sequencing can replace Sanger sequencing in clinical diagnostics. *Hum. Mutat.*, **34**, 1035–1042.
67. Singh, N.A., Westenskow, P., Charlier, C., Pappas, C., Leslie, J., Dillon, J., Anderson, V.E., Sanguinetti, M.C. and Leppert, M.F. (2003) KCNQ2 and KCNQ3 potassium channel genes in benign familial neonatal convulsions: expansion of the functional and mutation spectrum. *Brain*, **126**, 2726–2737.
68. Berkovic, S.F., Heron, S.E., Giordano, L., Marini, C., Guerrini, R., Kaplan, R.E., Gambardella, A., Steinlein, O.K., Grinton, B.E., Dean, J.T. *et al.* (2004) Benign familial neonatal-infantile seizures: characterization of a new sodium channelopathy. *Ann. Neurol.*, **55**, 550–557.
69. Lunter, G. and Goodson, M. (2011) Stampy: a statistical algorithm for sensitive and fast mapping of Illumina sequence reads. *Genome Res.*, **21**, 936–939.
70. Pagnamenta, A.T., Lise, S., Harrison, V., Stewart, H., Jayawant, S., Quaghebeur, G., Deng, A.T., Murphy, V.E., Akha, E.S., Rimmer, A. *et al.* (2012) Exome sequencing can detect pathogenic mosaic mutations present at low allele frequencies. *J. Hum. Genet.*, **57**, 70–72.
71. Wang, K., Li, M. and Hakonarson, H. (2010) ANNOVAR: functional annotation of genetic variants from high-throughput sequencing data. *Nucleic Acids Res.*, **38**, e164.
72. Conrad, D.F., Keebler, J.E., DePristo, M.A., Lindsay, S.J., Zhang, Y., Casals, F., Idaghdour, Y., Hartl, C.L., Torroja, C., Garimella, K.V. *et al.* (2011) Variation in genome-wide mutation rates within and between human families. *Nat. Genet.*, **43**, 712–714.
73. Davydov, E.V., Goode, D.L., Sirota, M., Cooper, G.M., Sidow, A. and Batzoglou, S. (2010) Identifying a high fraction of the human genome to be under selective constraint using GERP++. *PLoS Comput. Biol.*, **6**, e1001025.
74. Pollard, K.S., Hubisz, M.J., Rosenbloom, K.R. and Siepel, A. (2010) Detection of nonneutral substitution rates on mammalian phylogenies. *Genome Res.*, **20**, 110–121.
75. Siepel, A., Bejerano, G., Pedersen, J.S., Hinrichs, A.S., Hou, M., Rosenbloom, K., Clawson, H., Spieth, J., Hillier, L.W., Richards, S. *et al.* (2005) Evolutionarily conserved elements in vertebrate, insect, worm, and yeast genomes. *Genome Res.*, **15**, 1034–1050.
76. Chen, W., Han, Y., Chen, Y. and Astumian, D. (1998) Electric field-induced functional reductions in the K+ channels mainly resulted from supramembrane potential-mediated electroconformational changes. *Biophys. J.*, **75**, 196–206.
77. Watanabe, R., Inoue, N., Westfall, B., Taron, C.H., Orlean, P., Takeda, J. and Kinoshita, T. (1998) The first step of glycosylphosphatidylinositol biosynthesis is mediated by a complex of PIG-A, PIG-H, PIG-C and GPI1. *EMBO J.*, **17**, 877–885.
78. Ashida, H., Hong, Y., Murakami, Y., Shishioh, N., Sugimoto, N., Kim, Y.U., Maeda, Y. and Kinoshita, T. (2005) Mammalian PIG-X and yeast Pbn1p are the essential components of glycosylphosphatidylinositol-mannosyltransferase I. *Mol. Biol. Cell.*, **16**, 1439–1448.
79. O'Roak, B.J., Vives, L., Fu, W., Egertson, J.D., Stanaway, I.B., Phelps, I.G., Carvill, G., Kumar, A., Lee, C., Ankenman, K. *et al.* (2012) Multiplex targeted sequencing identifies recurrently mutated genes in autism spectrum disorders. *Science*, **338**, 1619–1622.

PIGA mutations cause early-onset epileptic encephalopathies and distinctive features

Mitsuhiro Kato, MD, PhD*
Hirotomo Saitsu, MD, PhD*
Yoshiko Murakami, MD, PhD*
Kenjiro Kikuchi, MD
Shuei Watanabe, MD
Mizue Iai, MD
Kazushi Miya, MD
Ryuki Matsuura, MD
Rumiko Takayama, MD
Chihiro Ohba, MD
Mitsuko Nakashima, MD, PhD
Yoshinori Tsurusaki, PhD
Noriko Miyake, MD, PhD
Shin-ichiro Hamano, MD
Hitoshi Osaka, MD, PhD
Kiyoshi Hayasaka, MD, PhD
Taroh Kinoshita, PhD
Naomichi Matsumoto, MD, PhD

ABSTRACT

Objective: To investigate the clinical spectrum caused by mutations in *PIGA* at Xp22.2, which is involved in the biosynthesis of the glycosylphosphatidylinositol (GPI) anchor, among patients with early-onset epileptic encephalopathies (EOEEs).

Methods: Whole-exome sequencing was performed as a comprehensive genetic analysis for a cohort of 172 patients with EOEEs including early myoclonic encephalopathy, Ohtahara syndrome, and West syndrome, and *PIGA* mutations were carefully investigated.

Results: We identified 4 *PIGA* mutations in probands showing early myoclonic encephalopathy, West syndrome, or unclassified EOEE. Flow cytometry of blood granulocytes from patients demonstrated reduced expression of GPI-anchored proteins. Expression of GPI-anchored proteins in *PIGA*-deficient JY5 cells was only partially or hardly restored by transient expression of PIGA mutants with a weak TATA box promoter, indicating a variable loss of PIGA activity. The phenotypic consequences of *PIGA* mutations can be classified into 2 types, severe and less severe, which correlate with the degree of PIGA activity reduction caused by the mutations. Severe forms involved myoclonus and asymmetrical suppression bursts on EEG, multiple anomalies with a dysmorphic face, and delayed myelination with restricted diffusion patterns in specific areas. The less severe form presented with intellectual disability and treatable seizures without facial dysmorphism.

Conclusions: Our study confirmed that *PIGA* mutations are one genetic cause of EOEE, suggesting that GPI-anchor deficiencies may be an underlying cause of EOEE. ***Neurology*® 2014;82:1587–1596**

GLOSSARY

ADC = apparent diffusion coefficient; **cDNA** = complementary DNA; **DWI** = diffusion-weighted image; **EME** = early myoclonic encephalopathy; **EOEE** = early-onset epileptic encephalopathy; **GPI** = glycosylphosphatidylinositol; **GPI-AP** = glycosylphosphatidylinositol-anchored protein; **OS** = Ohtahara syndrome; **WES** = whole-exome sequencing.

Early-onset epileptic encephalopathies (EOEEs) present with developmental impairment and disastrous seizures starting in early infancy with a mode of age dependency. Ohtahara syndrome (OS) and early myoclonic encephalopathy (EME), both of which show a distinctive EEG finding called suppression-burst pattern, are neonatal EOEEs. Genetic approaches have revealed some of the genes that are mutated in EOEEs. For instance, *ARX*, *STXBP1*, *CASK*, *KCNQ2*, and *SCN2A* are mutated in OS,[1–5] while *ARX*, *CDKL5*, and *SPTAN1* mutations cause West syndrome or infantile spasms.[6–8]

Mutations in 8 genes (*PIGA*, *PIGM*, *PIGN*, *PIGV*, *PIGL*, *PIGO*, *PIGT*, and *PGAP2*) involved in the biosynthesis of the glycosylphosphatidylinositol (GPI) anchor, a glycolipid structure embedded in the plasma membrane that attaches to hundreds of cell-surface proteins, have been identified in patients with a variety of multiple congenital anomalies, intellectual disability, and epileptic seizures.[9–16] Somatic mutations of *PIGA* at Xp22.2, which is involved in

Correspondence to Dr. Kato: mkato@med.id.yamagata-u.ac.jp or Dr. Saitsu: hsaitsu@yokohama-cu.ac.jp

Supplemental data at Neurology.org

*These authors contributed equally to this work.

From the Department of Pediatrics (M.K., K.H.), Yamagata University Faculty of Medicine, Yamagata; Department of Human Genetics (H.S., C.O., M.N., Y.T., N. Miyake, N. Matsumoto), Yokohama City University Graduate School of Medicine, Yokohama; Department of Immunoregulation (Y.M., T.K.), Research Institute for Microbial Diseases, and WPI Immunology Frontier Research Center, Osaka University, Suita; Division of Neurology (K.K., R.M., S.-i.H.), Saitama Children's Medical Center, Saitama; Division of Neurology (S.W.), Miyagi Children's Hospital, Sendai; Division of Neurology (M.I., H.O.), Clinical Research Institute, Kanagawa Children's Medical Center, Yokohama; Department of Pediatrics (K.M.), Graduate School of Medicine and Pharmaceutical Sciences, University of Toyama; Department of Pediatrics (R.T.), Aomori Prefectural Central Hospital, Aomori; and Department of Pediatrics (H.O.), Jichi Medical School, Tochigi, Japan.

Go to Neurology.org for full disclosures. Funding information and disclosures deemed relevant by the authors, if any, are provided at the end of the article.

the first step of the GPI biosynthesis, are responsible for paroxysmal nocturnal hemoglobinuria, and its germline mutation, were recently identified in a family with multiple congenital anomalies, neonatal seizures, and a poor prognosis.[11] At least 2 of 3 patients in this family showed severe myoclonic seizures with suppression bursts on EEG, strongly suggesting EME. The known mutations in EME prompted us to investigate *PIGA* in the EOEE patient cohort including EME and OS. We identified *PIGA* mutations in 5 patients from 4 families with EOEEs and present the clinical phenotypes of the patients and functional effects of the mutations in this study.

METHODS Patients. A total of 172 patients with EOEEs (2 with EME, 50 with OS, 50 with West syndrome or infantile spasms, 7 with malignant migrating partial seizures in infancy, and 63 with unclassified epileptic encephalopathy with an age at onset of <1 year; 90 male and 82 female patients) were analyzed by whole-exome sequencing (WES), and *PIGA* mutations were carefully investigated using WES data.

Patients had been mainly enrolled in the Japanese collaborative study for EOEE since 2003. The diagnosis was made based on clinical features and characteristic EEG patterns. Patients with mutations in *STXBP1*, *ARX*, *KCNQ2*, *SCN1A*, *SCN2A*, *KCNT1*, *CDKL5*, *CASK*, or *MECP2*, which were detected by high-resolution melting analysis, target capture analysis, direct sequencing analysis, or WES, were excluded from the study.

Whole-exome sequencing. Patient and parental genomic DNA was obtained from peripheral blood leukocytes using standard methods. DNA was captured using the SureSelectXT Human All Exon Kit (v4 or v5; Agilent Technologies, Santa Clara, CA) and sequenced on an Illumina HiSeq2000 (Illumina, San Diego, CA) with 101–base pair paired-end reads. Image analysis and base calling were performed using sequence control software real-time analysis and CASAVA software v1.8 (Illumina). Exome data processing, variant calling, and variant annotation were performed as previously described.[17–19] All novel mutations in *PIGA* were verified using Sanger sequencing.

Fluorescence-activated cell sorting analysis. Surface expression of GPI-anchored proteins (GPI-APs) was determined by staining cells with Alexa 488–conjugated inactivated aerolysin (FLAER; Protox Biotech, Victoria, Canada) and appropriate primary antibodies, namely, mouse anti-CD59 (5H8), DAF (IA10), CD16 (3G8), CD24 (ML5), and CD48 (BJ40), followed by a phycoerythrin-conjugated anti-mouse immunoglobulin G antibody (3G8, ML5, BJ40, and secondary antibodies; BD Biosciences, Franklin Lakes, NJ). Cells were analyzed by flow cytometry (Cant II; BD Biosciences).

Functional analysis using *PIGA*-deficient B lymphoblastoid cells (JY5). FLAG-tagged human *PIGA* complementary DNA (cDNA) and mutant cDNAs, generated by site-directed mutagenesis, were subcloned into the pMEoriP vector, a strong promoter (SRα)-driven vector or pTAoriP, a weak TATA box promoter-driven vector. Plasmid DNA was transfected by electroporation into *PIGA*-deficient JY5 cells. Expression of GPI-APs was analyzed by fluorescence-activated cell sorting. PIGA protein levels in transfected cells were determined by Western blotting using an anti-FLAG antibody (M2; Sigma, St. Louis, MO).

Standard protocol approvals, registrations, and patient consents. The experimental protocols were approved by the institutional review boards for ethical issues of Yamagata University Faculty of Medicine, Yokohama City University School of Medicine, and Osaka University, Japan. Written informed consent was obtained from all individuals and/or their families in compliance with relevant Japanese regulations. Permission for publishing photographs was also obtained from the parents.

RESULTS Identification of *PIGA* mutations. No mutations were found in *SLC25A22*, which had been reported in a family of EME.[20] We identified 4 hemizygous *PIGA* mutations in 3 sporadic patients and 2 siblings with EOEE. One mutation (c.1234C>T [p.R412X]) had previously been reported,[11] while the other 3 were novel missense mutations (c.230G>T [p.R77L], c.616A>T [p.I206F], and c.355C>T [p.R119W]). DNA from the mother of patient 1 (p.R412X) was unavailable. Three missense mutations were maternally inherited. All mutations were absent from the 6,500 exomes of the National Heart, Lung, and Blood Institute exome project and our 573 in-house control exomes (281 male and 292 female patients). All 4 mutations occurred at evolutionarily conserved amino acids (figure 1A) and were predicted to be highly damaging to the protein structure by SIFT, PolyPhen-2, and MutationTaster (table e-1 on the *Neurology*® Web site at Neurology.org), which supported their pathogenicity.

Clinical features of patients with the *PIGA* mutation. The clinical information of individuals with a *PIGA* mutation is summarized in table 1, and their facial appearances and representative brain images are shown in figures 1 and 2, respectively. EEG findings (figure e-1) and detailed case reports (appendix e-1) are available in supplemental data. Two patients were associated with polyhydramnios. Birth weight and length were normal in 3 patients (patients 2, 3, and 5) who were born at term, but the other 2 who were born at preterm showed higher (patient 1) or lower (patient 4) birth weights than normal. Three patients with the severe phenotype (patients 1, 2, and 5) showed facial dysmorphisms (figure 1, B and C), including a depressed nasal bridge, short anteverted nose, downturned corners of the mouth, and high arched palate. Patient 1 also showed bilateral vesicoureteral reflux of the most severe grade V. In addition, brain MRI demonstrated a thin corpus callosum and delayed myelination in these patients. Of interest, abnormally high signals on diffusion-weighted images (DWIs) and low signals on the apparent diffusion coefficient (ADC) map at the brainstem, basal ganglia, thalamus, and deep white matter were found in patients 1, 2, and 5 (figure 2, A–D and M–Q). By

Figure 1 *PIGA* mutations in patients with epileptic encephalopathy and dysmorphic features

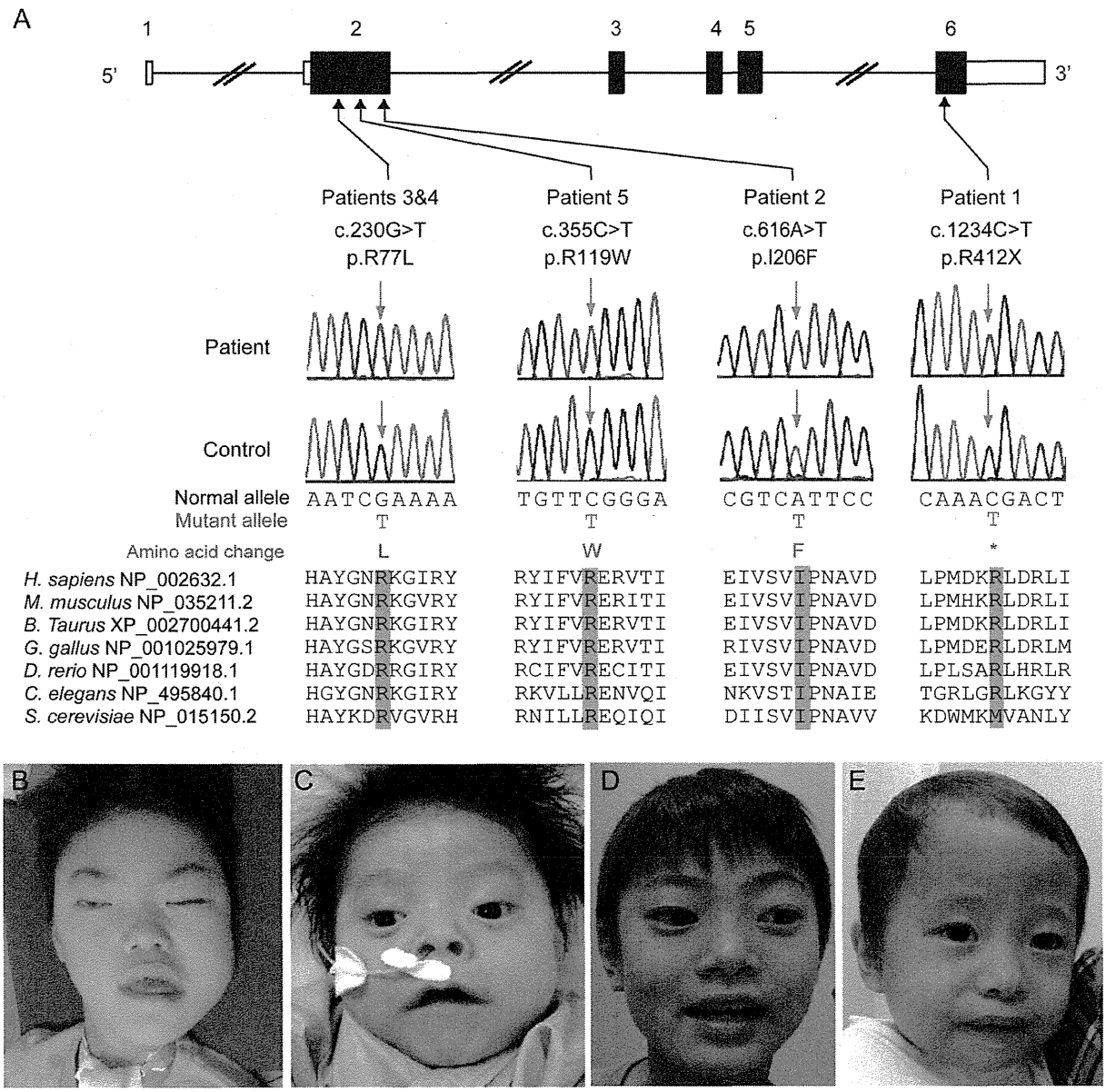

(A) Schematic presentation of *PIGA* genomic structure. Mutations are indicated based on the transcript variant 1 (GenBank accession number, NM_002641.3). Untranslated regions and coding regions are shown as white and black rectangles, respectively. All mutations occurred at evolutionarily conserved amino acids. Orthologous sequences were aligned using the CLUSTALW Web site. (B–E) Facial appearance of patients 2, 3, 4, and 5. Both patients 2 (B) and 5 (C) show distinct facial features, such as upslanting palpebral fissures, depressed nasal bridge, short anteverted nose, triangular mouth with downturned corners, and high arched palate, compared with patients 3 (D) and 4 (E) with no dysmorphic facial features.

contrast, 2 brothers with a less severe phenotype (patients 3 and 4) showed neither dysmorphic signs nor abnormalities in brain MRI (figure 2, E–L).

The first seizures started between 1 and 7 months of age, and tonic or myoclonic seizures occurred in all patients. Seizures of patients 1, 2, and 5 were refractory to antiepileptic medications, but topiramate was effective for the seizures of patient 3. The initial EEG showed a suppression burst in patient 1; patients 2 and 5 first demonstrated hypsarrhythmia, followed by a symmetrical or asymmetrical suppression burst later (figure e-1). Serum alkaline phosphatase levels were elevated in patients 2 and 5. No patients showed anemia or hemoglobinuria. All patients showed profound intellectual disability, and patients 1, 2, and 5 were bedridden with severe motor disturbance.

Flow cytometry. We analyzed the surface expression of various GPI-APs on patient granulocytes using flow

Table 1 **Clinical summary of patients with a *PIGA* mutation**

	Patients						
	IV-2	IV-4	1	2	3	4	5
Familial or sporadic	Familial or sporadic	Familial (brother)	Sporadic	Sporadic	Familial (proband)	Familial (brother)	Sporadic
Mutation	c.1234C>T (p.R412X)	c.1234C>T (p.R412X)	c.1234C>T (p.R412X)	c.616A>T (p.I206F)	c.230G>T (p.R77L)	c.230G>T (p.R77L)	c.355C>T (p.R119W)
Current age	Died at 11 wk	Died at 10 wk	6 y	10 y	8 y	18 mo	15 mo
Sex	M	M	M	M	M	M	M
Clinical diagnosis			Ohtahara syndrome, early myoclonic encephalopathy, Schinzel-Giedion syndrome	West syndrome with hypomyelination	Early-onset epileptic encephalopathy	Early-onset epileptic encephalopathy	West syndrome
Polyhydramnios	–	+	+	–	–	–	+
Gestation, wk	Full term	35	33	40	38	36	39
Birth weight, g	3,540	3,500	2,857	3,566	2,715	1,896	3,468
Birth length, cm	53.5	48	42.0	50	50	ND	47
Birth head circumference, cm	37	35.5	33.2	ND	32.5	ND	33.5
Facial dysmorphism	+	+	+	+	–	–	+
Vesicoureteral reflux	+	ND	+	ND	–	–	ND
Joint contractures	+	+	+	+	–	–	–
Hypotonia	+	+	+	–	–	–	+
Hyperreflexia	+	+	ND	–	–	–	+
Seizure onset	Neonate	Neonate	1 mo	3 mo	7 mo	7 mo	3 mo
Seizure types	Myoclonic	Severe myoclonic	Tonic seizures followed by frequent myoclonus	Myoclonus or epileptic spasm-like movement	Tonic seizures, secondarily generalized seizures	Tonic or clonic	Myoclonic seizures, tonic spasms
EEG findings	Suppression burst	Suppression burst	Suppression burst at neonatal period	Hypsarrhythmia at 3 mo, periodic bursts of multifocal epileptic discharges similar to suppression-burst pattern at 10 y	Normal at 7 mo, irregular spike and slow wave and multifocal spikes at 2 and 5 y	Normal at 7 mo	Hypsarrhythmia at 3 mo, suppression burst at 5 mo
Seizure prognosis	Intractable	Intractable	Intractable	Intractable	Seizure-free at 3 y with TPM	Seizure-free at 15 mo	Intractable
Development	Early death	Early death	Hypotonic quadriplegia, profound intellectual disability	Spastic quadriplegia, profound intellectual disability	Profound intellectual disability with autism, but no motor disturbance	Moderate intellectual disability, but no motor disturbance	Hypotonic quadriplegia, profound intellectual disability
Thin corpus callosum	+	+	+	+	–	–	+ (at 9 mo)
White matter immaturity	+	+	+	+	–	–	+ (at 9 mo)
Restricted diffusion pattern	ND	ND	+	+	–	–	+
Elevated serum alkaline phosphatase	ND	+	ND	+	–	–	+

Abbreviations: ND = not determined; TPM = topiramate.

Figure 2 **Brain MRIs of patients with *PIGA* mutations**

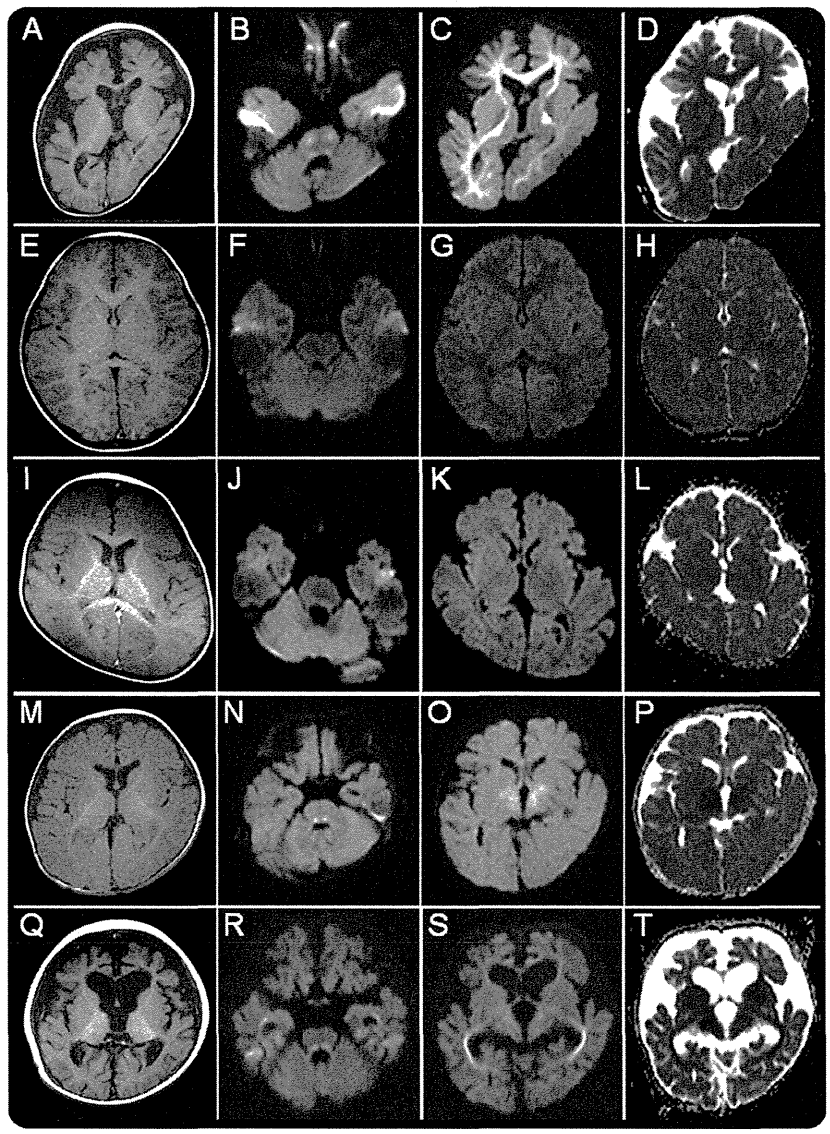

MRIs of patient 2 at 6 months (A) and 7 years (B–D), patient 3 at 3 years (E–H), patient 4 at 7 months (I–L), and patient 5 at 3 months (M–P) and 9 months (Q–T) of age. Left panels (A, E, I, M, Q) show axial T1-weighted images, the 2 middle panels (B, C, F, G, J, K, N, O, R, S) show axial diffusion-weighted images (DWIs), and right panels (D, H, L, P, T) show apparent diffusion coefficient (ADC) maps. Patient 2 and patient 5 at 9 months show cortical atrophy and enlarged ventricles. Note the high signals on DWI in the pontine tegmentum and deep white matter, particularly the optic radiation, of patients 2 and 5 in accordance with their age. The ADC map demonstrated decreased ADC within the same lesion. Patients 3 and 4 show normal images.

cytometry (figure 3). In all 5 patients, the surface expression of CD16 was severely decreased (from 5% to 15% of normal levels). Patient 1, with the most severe clinical symptoms, had a tendency to show reduced expression of other GPI-APs, such as CD24 and FLAER (figure 4A). Because *PIGA* is an X-linked gene and one allele is inactivated during early embryogenesis in female patients, patient mothers would be functionally mosaic for GPI-AP expression. Granulocytes from the mother of patients 3 and 4 showed a significantly decreased expression of CD16 (figure e-2, upper panels), whereas those from the mother of patient 5 showed normal expression (figure e-2, lower panels). The mothers appeared to have no neurologic disorder, suggesting that GPI-sufficient cells may preferentially proliferate in the brain during early embryogenesis.

Functional analysis. *PIGA* cDNAs bearing patient mutations were functionally analyzed by transfecting them into *PIGA*-deficient B lymphoblastoid cells (JY5) and measuring the surface expression of GPI-APs.

Figure 3 **Flow cytometry of granulocytes**

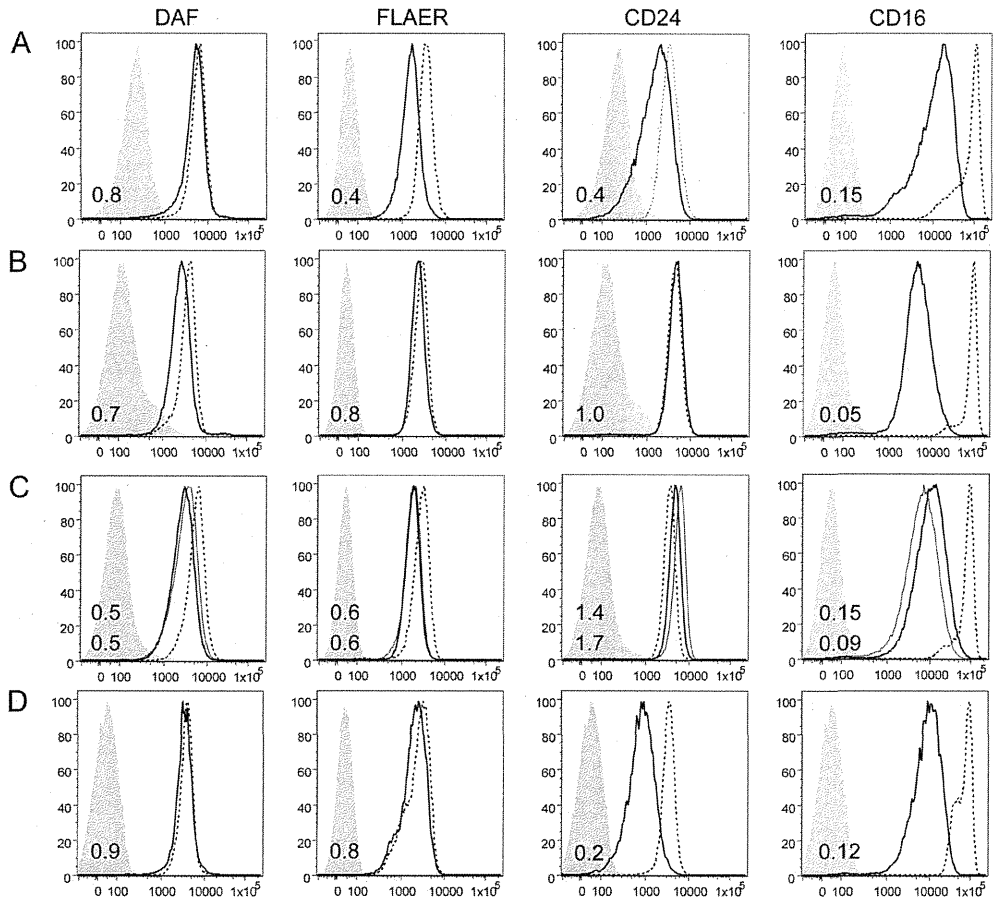

Flow cytometry of patient 1 (R412X) (A), patient 2 (I206F) (B), patients 3 and 4 (2 brothers, R77L) (C), and patient 5 (R119W) (D). In all families, the surface expression of various glycosylphosphatidylinositol-anchored proteins on patient granulocytes (solid lines; patients 3 and 4 are shown in C as thin and thick lines, respectively) was severely decreased compared with the normal control (dotted lines). Light shadows represent isotype controls. Mean fluorescent intensities of each sample against a normal control are shown in each panel (upper, patient 4; lower, patient 3 in C).

When strong promoter (SRα)-driven constructs were used, R412X mutant cDNA completely restored the surface expression of CD59, DAF, and CD48, whereas R412 truncated cDNA had no activity (figure 4A), suggesting that a small amount of full-length PIGA protein was generated by readthrough of a stop codon. When weak promoter-driven constructs (pTA) were used instead, R412X cDNA could not restore the surface expression of GPI-APs, whereas it was completely restored by wild-type cDNA (figure 4B). Similarly, the strong promoter (SRα)-driven I206F and R77L mutant PIGAs completely restored the surface expression of GPI-APs, whereas the weak promoter-driven mutant constructs only partially restored this (figure 4, C–F). Levels of expressed mutant PIGA proteins were similar to or even higher than wild-type levels (figure e-3). A faint band representing full-length PIGA protein harboring R412X could be detected (figure e-3, lane 4), which was consistent with the functional analysis. From these results, we concluded that these mutations affect the PIGA activity leading to inherited GPI deficiency.

DISCUSSION We have identified 4 *PIGA* mutations in 172 probands from a variety of EOEE-affected families, such as EME (n = 1), West syndrome (n = 2), and unclassified EOEE in a sibling. Myoclonus and suppression burst on EEG were recognized in 2 patients with West syndrome and the patient with EME in our cohort, as well as the previously reported family.[11] Indeed, myoclonus and suppression burst on EEG appear to be characteristic features for patients with a *PIGA* mutation.

Other clinical features such as polyhydramnios, facial dysmorphism, joint contractures, hypotonia, and severe developmental delay are recurrently seen in patients with *PIGA* mutations. A previous report of 3 patients with the same nonsense mutation,

Figure 4 **Functional analysis of the mutant PIGA**

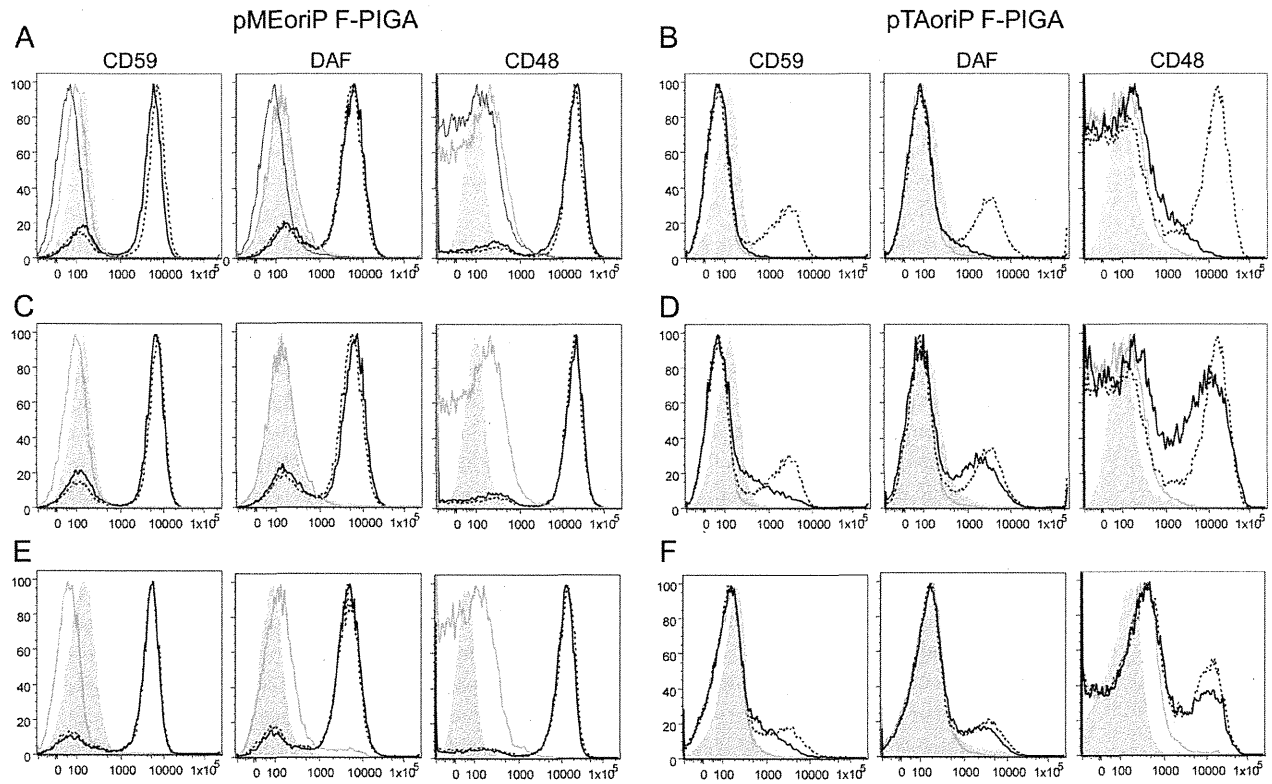

JY5 cells were transiently transfected with pMEoriP (strong SRα promoter-driven, Epstein-Barr [EB] virus origin-containing vector) (panels A, C, and E) or pTAoriP F-PIGA (weak TATA box promoter-driven, EB virus origin-containing vector) (panels B, D, and F) bearing various FLAG-tagged PIGA complementary DNAs. Restoration of the surface expression of CD59, DAF, and CD48 was assessed 2 days later by flow cytometry. Dotted lines represent wild-type PIGA, thick lines represent mutant PIGA, thin lines represent truncated PIGA, and shadows represent isotype controls. (A) Strong promoter-driven R412X PIGA (thick lines) completely rescued the expression of glycosylphosphatidylinositol-anchored proteins (GPI-APs) similar to wild-type PIGA (dotted lines), whereas R412-truncated PIGA (thin lines) had no activity. (B) Weak promoter-driven R412X PIGA (thick lines) did not rescue the surface expression of GPI-APs, whereas wild-type PIGA (dotted lines) did. (C) Strong promoter-driven I206F PIGA (thick lines) completely rescued the expression of GPI-APs similar to wild-type PIGA (dotted lines). (D) Weak promoter-driven I206F PIGA (thick lines) did not rescue the surface expression of GPI-APs, whereas wild-type PIGA (dotted lines) did. (E) Strong promoter-driven R77L PIGA (thick lines) completely rescued the expression of GPI-APs similar to wild-type PIGA (dotted lines). (F) Weak promoter-driven R77L PIGA (thick lines) did not rescue the surface expression of CD59, whereas wild-type PIGA (dotted lines) did.

R412X,[11] as patient 1 in our cohort showed similar or more severe clinical features, such as a large occipitofrontal circumference at birth, early-onset intractable seizures, and severe respiratory failure leading to early death or mechanical ventilation. Complete disruption of the *PIGA* gene results in early embryonic lethality in male mice, while heterozygous female mice have late embryonic lethality, insufficient closure of the neural tube, and a cleft palate.[21] In the present study, a reduced but definite expression of GPI-APs in the granulocytes of patients with R412X and a complete restoration of GPI-AP surface expression by the transfection of R412X mutant cDNA under the control of a strong promoter suggest that small amounts of full-length PIGA protein were generated by the read-through of a stop codon because the cDNA truncated at R412 showed no activity.

The siblings with the *PIGA* p.R77L mutation demonstrated milder clinical symptoms compared with patients with other *PIGA* mutations. They showed neither dysmorphisms nor severe motor disturbance, the onset of their seizures was relatively late, and the findings of their initial EEG and brain MRI were normal. Flow cytometry only revealed a decreased expression of CD16, which contrasts with the more severe phenotype of patient 1 and associated decreased levels of CD16, FLAER, and CD24. According to the functional study using *PIGA*-deficient B lymphoblasts transfected with a weak promoter-driven mutant *PIGA*, the activity of the R77L mutant was higher than that of other mutants. Thus, the phenotype severity appears to correlate with genotype and the residual functional activity of the PIGA protein.

Patients 2 and 5 showed peculiarly high signals on DWI at the specific areas of the brainstem, basal ganglia, thalamus, and deep white matter, particularly the optic radiation as previously reported in patient 1.[22] Although delayed myelination and the volume loss of

white matter including a thin corpus callosum, mild brain atrophy, and mild cerebellar hypoplasia are frequently seen in patients with mutations in other genes involved in the biosynthesis of the GPI anchor, such as *PIGN*, *PGAP2*, *DPM1*, and *DPM2*,[10,15,23,24] high signals on DWI have never been reported. In addition, the ADC map showed adversely low or decreased signals, suggesting restricted water diffusion. This pattern (a high DWI signal and low ADC values) can be seen in patients with specific metabolic disorders, such as nonketotic hyperglycinemia, phenylketonuria, maple syrup urine disease, Leigh encephalopathy, infantile neuroaxonal dystrophy, Wilson disease, metachromatic leukodystrophy, and Canavan disease.[25] Indeed, metabolic disorders, particularly nonketotic hyperglycinemia, are strongly associated with EME, which is common in patients with *PIGA* mutations. A brain MRI of a patient in early infancy with a recently reported *PIGO* deficiency also showed hypomyelination and abnormally high signals in T2-weighted images from the bilateral basal ganglia to the brainstem.[26] While the pathologic mechanism for restricted diffusion patterns in specific areas is unknown, this finding may be useful to screen patients with a GPI deficiency.

Patients with the severe type of *PIGA* mutation showed both an asymmetrical and symmetrical pattern of suppression burst on EEG in this study. The suppression burst pattern is characteristic for 2 types of EOEE, OS and EME, and most patients of both disorders show a symmetrical pattern. The asymmetrical pattern has been reported in patients with agenesis of the corpus callosum such as Aicardi syndrome,[27] and *KCNQ2* mutations.[4] All 3 patients with the asymmetrical suppression burst in the present study also showed white matter immaturity with a thin corpus callosum and abnormally high signals in deep white matter on DWI. These data indicate a disturbed connectivity of the bilateral hemisphere in patients with *PIGA* mutations. The adverse advancement of the EEG findings from hypsarrhythmia to suppression burst in our cases, which is usually observed in neonates, might reflect the retrogression of brain function, which is also seen in the progression of brain atrophy.

Patient 1 showed severe hydronephrosis caused by the vesicoureteral reflux and hepatoblastoma, so a diagnosis of Schinzel-Giedion syndrome was made. This is an autosomal dominant disorder characterized by severe developmental delay, distinctive facial features with a prominent forehead, midface retraction, short, upturned nose, and either hydronephrosis or typical skeletal malformations, such as sclerotic skull base, wide occipital synchondrosis, increased cortical density or thickness, and broad ribs.[28] *SETBP1* mutations have been reported in patients with Schinzel-Giedion syndrome[29] but were not identified in our patient. Because of the phenotypic similarities between patients with *PIGA* mutation and those with Schinzel-Giedion syndrome, we suggest that patients with Schinzel-Giedion syndrome with no *SETBP1* mutations should undergo genetic analysis of their *PIGA* gene or other genes involved in the biosynthesis of the GPI anchor.

Patients with mutations in *PIGL*, *PIGM*, *PIGN*, *PIGO*, *PIGT*, *DPM2*, and *MPDU1* often die in early childhood.[9,12,14–16,23,30] While pneumonia is the main cause of death in these patients, intractable seizures, which rigorously worsen the prognosis of life expectancy and cognitive function, frequently occur. It is of interest that the targeted agents butyrate and pyridoxine were reported to be effective for seizure treatment in patients with *PIGM* or *PIGO* mutation, respectively.[26,31] However, patient 5 in this study did not respond to pyridoxine. The study of more patients will facilitate the establishment of personalized treatment methods for patients with GPI deficiencies.

Our study demonstrated that mutations in *PIGA* are causative for a variety of EOEEs, particularly for patients with myoclonus and asymmetrical suppression burst on EEG. Multiple anomalies with facial dysmorphism resembling Schinzel-Giedion syndrome, delayed myelination with restricted diffusion patterns at the brainstem, and deep white matter are key findings in a severe form in patients with *PIGA* mutations. Nevertheless, a wide range of clinical phenotypes of *PIGA* mutations should be kept in mind, including the less severe forms involving intellectual disability and treatable seizures without facial dysmorphism.

AUTHOR CONTRIBUTIONS

Mitsuhiro Kato: study concept and design, analysis of the clinical data, interpretation of the data, and drafting/revising of the manuscript. Hirotomo Saitsu: study concept and design, analysis of the genetic data, interpretation of the data, and drafting/revising of the manuscript. Yoshiko Murakami: study concept and design, analysis of the biological data, interpretation of the data, and drafting/revising of the manuscript. Kenjiro Kikuchi, Shuei Watanabe, Mizue Iai, Kazushi Miya, Ryuki Matsuura, and Rumiko Takayama: analysis of the clinical data and sample collection. Chihiro Ohba, Mitsuko Nakashima, Yoshinori Tsurusaki, and Noriko Miyake: analysis of the genetic data. Shin-ichiro Hamano and Hitoshi Osaka: analysis of the clinical data and sample collection. Kiyoshi Hayasaka: analysis of the clinical data and revising of the manuscript. Taroh Kinoshita: analysis of the biological data, interpretation of the data, and drafting/revising of the manuscript. Naomichi Matsumoto: study concept and design, analysis of the genetic data, interpretation of the data, and drafting/revising of the manuscript.

ACKNOWLEDGMENT

The authors are grateful to the patients and their families for their participation in this study. The authors thank Keiko Tanaka, Kana Miyanagi, Nobuko Watanabe, and Kiyomi Masuko for their technical assistance.

STUDY FUNDING

This study was supported by the Ministry of Health, Labour and Welfare of Japan (25140101, 24133701,11103577, 11103340, 10103235), a Grant-in-Aid for Scientific Research (A), (B), and (C) from the Japan